DESIGN AND PERFORMANCE OF A BENCH-SCALE STEAM FLUIDIZED GASIFIER FOR BIOMASS ANALYSIS

by

Brett Christensen

A thesis submitted to the faculty of
The University of Utah
in partial fulfillment of the requirements for the degree of

Master of Science

Department of Chemical Engineering

The University of Utah

August 2011

The University of Utah Graduate School

STATEMENT OF THESIS APPROVAL

The thesis of **Brett P. Christensen**

has been approved by the following supervisory committee members:

Kevin J. Whitty	, Chair	**6-10-2011** Date Approved
Terry A. Ring	, Member	**6-10-2011** Date Approved
Geoffrey D. Silcox	, Member	**6-10-2011** Date Approved

and by **JoAnn S. Lighty** , Chair of

the Department of **Chemical Engineering**

and by Charles A. Wight, Dean of The Graduate School.

ABSTRACT

Gasification has become an attractive technology that is capable of producing a rich syngas from a range of biomasses and other fuels. This syngas can then be further processed into liquid fuels through Fischer-Tropsch processes to provide an alternative to current fossil fuels or to provide local markets with a competitive fuel. The purpose of this study was to construct a four-inch bench scale fluidized bed gasifier to operate at a variety of stable conditions and to analyze the resulting syngas stream.

A sampling system was constructed from a Perma Pure dryer that consists of a single Nafion® tube capable of removing water vapor from the syngas stream while preserving the other gas compounds for analysis. A heated filter held at 250°F was installed before the dryer to remove particulate matter and condense tars, thus preserving the integrity of the dryer. Using this sampling system provided a higher quality gas stream for analysis than conventional methods. Carbon monoxide, hydrogen, carbon dioxide, methane, ethane, acetylene, ethylene, pentane, butane, propane, propylene, methyl mercaptan and five unknown compounds were identified by the Varian CP-4900 micro gas chromatograph. However, the gas stream did not contain any hydrogen sulfide, meaning there likely is still a problem with condensation and dissolution.

The reactor and sampling system have undergone a series of revisions to increase efficiency and accuracy from which a series of operating conditions could be tested.

Reactor temperature, biomass feed rate and types of fuel were selected as the operating variables. Findings were compared to theoretical calculations for concentration and trends. Results show that increasing temperature increases the production of hydrogen, volumetric flow rate and carbon conversion and decreases the production of hydrocarbons. Increasing the feed rate of biomass did not result in an increase in carbon monoxide or hydrogen, but did increase the volumetric flow rate and hydrocarbon production. Increased biomass feed rate also resulted in lower carbon conversion. Pine chips and switch grass were tested in the reactor and showed similar gas composition. However, further testing is needed on switch grass for a more complete analysis.

Tests show that the reactor is capable of producing a stable environment for a range of operating conditions and that the sampling system is capable of removing particulate matter and condensing tars. Further work on the reactor and sampling system can likely improve results.

TABLE OF CONTENTS

ACKNOWLEDGEMENTS

My sincerest thank you to Dr. Kevin Whitty, who has guided me in all aspects of this project from start to finish and enabled me to pursue my goals.

A special thank you to the staff of the Institute for Clean and Secure Energy (ICSE), particularly Dave Wagner, Dan Sweeney, Michael Burton and Eric Berg for their assistance.

The project received wonderful help from ThermoChem Recovery International, Inc. (TRI) and from the direction of Dr. Ravi Chandran.

Financial support for this project was provided by the United States Department of Energy under cooperative agreement DE-FG36-06GO18042. The subcontract was granted to the University of Utah by RTI International, which is also acknowledged for their contribution.

I also thank my wife, Genae, for her relentless support through long nights, her continued motivation and her incredible strength.

CHAPTER 1

INTRODUCTION

1.1 Field of Research

The search for suitable fossil fuel replacements is a challenging, motivating and captivating task that has been pursued for several decades (Dasappa et al., 2003). Many fields have been investigated, yielding opportunistic or ineffective technologies; often times, the successes have produced additional questions that require more research, resources and time. A suitable replacement has not been found and is still a major focus of the energy sector today. However, through the course of research, many industries have taken steps in applying appropriate technologies as immediate needs shift, guiding them to a narrower field of possible opportunities (Lee, 1996).

Fields of research have included natural gas, biomass, alcohols, biodiesel and even alternative methods for using the familiar fuels of today such as oxy-coal. One point that they all have in common is a high carbon content. These carbonaceous fuels offer a range of flexibility, availability and familiarity as current fuels and technology. As the demand of electricity and transportation fuels increases, it becomes more transparent that a suitable replacement must be renewable. Hence, the escalating interest in solar, thermal, wind and hydropower (Kelly, 2007).

Biomass is an intriguing alternative fuel as it is readily available in various forms throughout the world, is renewable and can be harnessed by agricultural means. Though biomass is a renewable source, the growth of some materials, such as wood, is a very long process and cannot be rapidly grown, while other crops are perennial, such as corn, straw and switch grass. Growth rate as well as availability must be considered while selecting a viable crop. It is also necessary to replace nutrients that are absorbed from the ground by plant growth or biomass production will be depleted over time.

Several methods exist for harnessing biomass energy, including gasification, pyrolysis, combustion and anaerobic digestion. A schematic of these methods and the subsequent processes and products is shown in Figure 1 (Bain, 2006). The most common method for the conversion of biomass is combustion. This process gives direct heating for electrical generation and remains a staple of survivability among third world countries. However, this method is only capable of harnessing about a third of the energy within biomass. Pyrolysis and anaerobic digestion are not as common as combustion but are used to produce charcoal, and to process waste products.

The advantage of gasification over combustion is the rich syngas that is produced, which can be processed further for a range of products. The syngas, mainly comprised of hydrogen and carbon monoxide, can be catalytically converted to alcohols, petroleum substitutes or other specialty chemicals via a Fischer-Tropsch process or separated for hydrogen or combusted (Maniatis, 2001). Gasification continues to be highlighted because of the attractiveness of producing liquid fuels used in transportation, manufacturing or used as precursors in the production of plastics and rubber. Additionally, several technologies exist for gasifying biomass and other fuels which adds

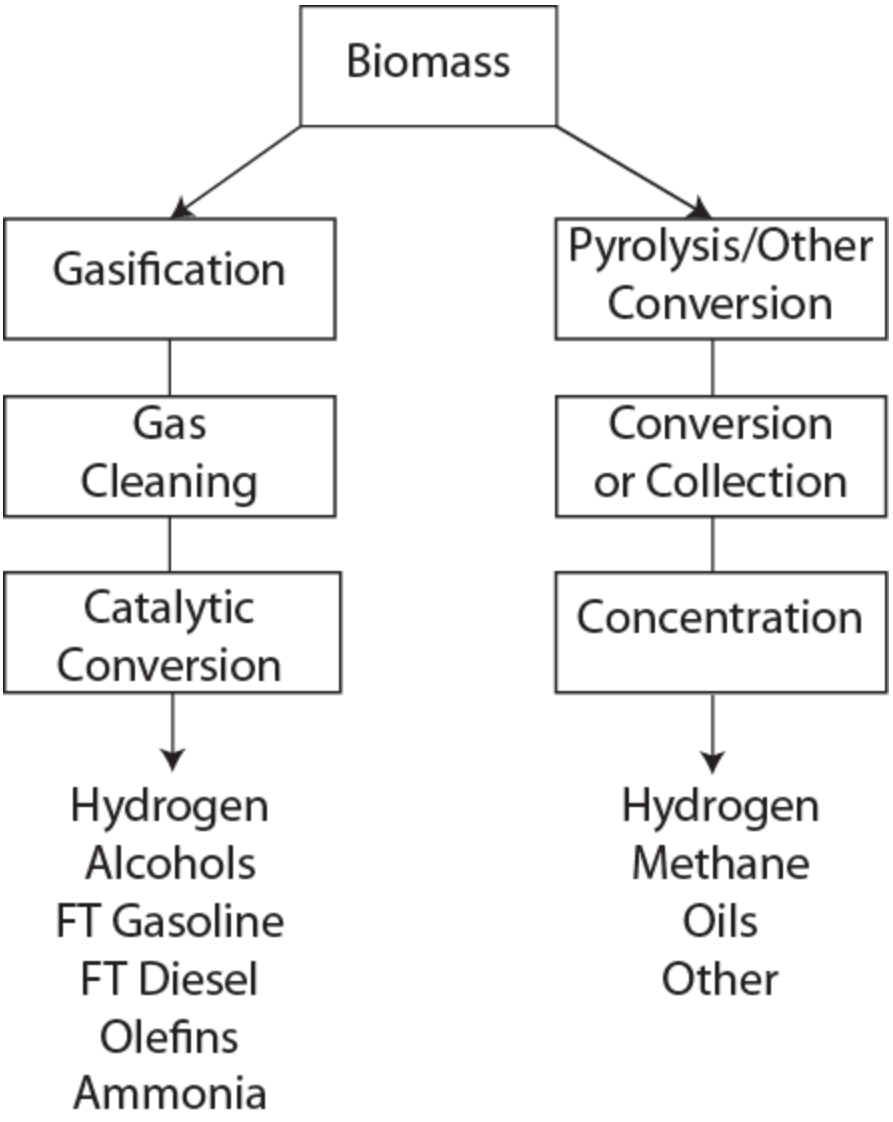

Figure 1. Common methods used for biomass processing and subsequent expected products (adapted from Bain, Richard, 2006).

to its versatility. The focus of this report is gasification of biomass by high temperature steam.

Gasification does not come without its own set of problems which must be overcome before the full potential is realized. With the syngas comes a host of other unknown and sometimes undesirable products such as tars, particulate matter and sulfur carrying species (Stiegel and Maxwell, 2001). Each of these byproducts has a negative effect on downstream processes or on the environment and must be removed before additional processing can occur. Eliminating these compounds requires further cleaning by filters, coolers and gas cleanup technology, adding to operating and capital costs. However, these obstacles can be minimized and overcome by additional research. One objective of this research is to remove these impurities from the sampling stream for improved syngas analysis.

1.2 Research Objectives

A better understanding of the behavior of sulfur containing molecules during steam gasification of biomass can yield a better approach to measuring and predicting their quantities throughout the different phases of gasification; more specifically, understanding the trends that appear by comparing various operating conditions and feed ratios to minimize their production. In order to achieve this, a suitable method for measuring sulfur containing molecules needs to be established and verified. The purpose of this work was to develop a method for measuring these components, verifying their presence and compositions and establish patterns. Key objectives to this research are outlined as follows:

1. Construct an experimental apparatus to give stable operating conditions for a variety of conditions which can produce the desired products for detailed analysis.
2. Develop a suitable method for measuring sulfur species despite high concentrations of water vapor.
3. Effectively remove the water vapor and other particulate matter without disturbing the syngas composition.
4. Analyze the data to establish the development and trends of the total syngas composition, including sulfur containing species and identify trends as functions of operating conditions.

CHAPTER 2

LITERATURE REVIEW

2.1 Gasification

Gasification is an intriguing and diverse field of study due to its complexity and variety of possible products. Some view the syngas as an alternative to present day fossil fuels for electrical production once operating costs become competitive (McKendry, 2002) or through the process of a catalytic system (e.g. Fischer-Tropsch), liquid fuels could be produced (Tijmensen et al., 2002). Various types of biomass can be used for gasification, which reduces the need and strain for a single crop of biomass for harvesting. In many instances, the availability and proximity of one or a few types of biomass to a local region can be attractive if it can reduce costs. All of these factors contribute to gasification's intrigue.

2.1.1 Steam and Air Gasification Overview

Grabowski (2004) defines gasification as thermal conversion of organic materials at elevated temperatures in the presence of steam into smaller constituent gases. Organic sources used in gasification are numerous and vary extensively in composition; however, the main component in gasifying fuels is carbon. Carbonaceous materials undergo gasification according to reactions (1)-(4) (Lv et al., 2004)

$$2C + O_2 = 2\text{CO} + 246.4\ \text{kJ} \quad (1)$$

$$C + O_2 = \text{CO}_2 + 408.8\ \text{kJ} \quad (2)$$

$$C + H_2O\ (g) = CO + H_2 - 131\ kJ \quad (3)$$

$$C + CO_2 = 2CO - 172\ kJ \quad (4)$$

Gasification reactions are classified as endothermic or exothermic and distinguished by their energy demands. Gasification via steam, the central focus of this project, is endothermic and is favorable at high temperatures. Since thermal energy cannot be created from steam gasification, liquid fuels can be produced from catalytic conversion of CO and H_2 or can be burned in a turbine for power generation. A schematic of possible thermal conversions of biomass is seen in Figure 2 (Knoef, 2001).

2.1.2 History of Gasification and Current Standing

Gasification technology has been in existence since the late 1800s and has fluctuated in popularity and use over the past 150 years (Grabowski, 2004). The peak of gasification usage was achieved during the 1940s, a time when politics and warfare depleted conventional fuel supplies and construction material. Gasification of coal and biomass was employed during that period due to a shortage of petroleum. The following decades saw a drastic reduction of interest in gasification as traditional fuel supplies returned, but it remained an important focus of research afterwards because usage involves broadly available resources. Gasification syngas can be used to produce liquid

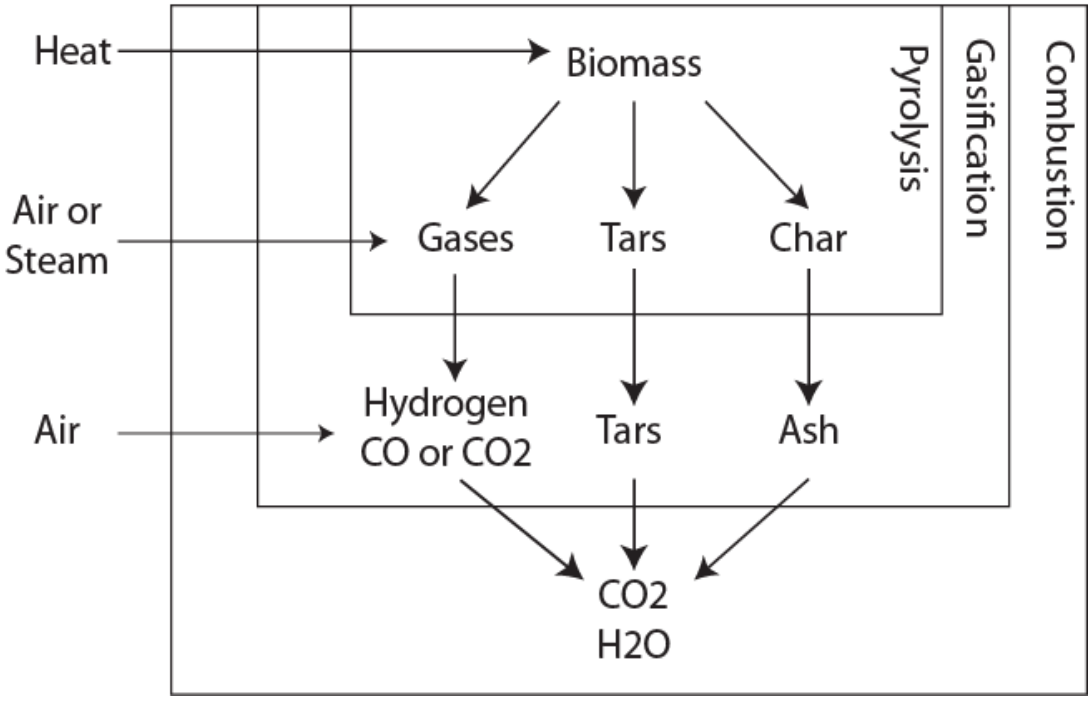

Figure 2. Schematic of the thermal conversion of biomass (adapted from Knoef, 2001).

fuels which have a high energy density, consumed for electricity generation or used in other chemical production (Schulz, 1999).

Large improvements have been made in gasification technology to improve efficiency (Ciferno and Marano, 2002), increase syngas production (Chaudhari et al., 2003) and tar reduction (Narvaez et al., 1997). However, some limitations continue to keep biomass gasification from becoming a common industrial source of fuels and energy. Obstacles include the amount of biomass available and its proximity to industrial complexes (Bridgwater, 1995), gas-cleaning systems for catalytic poisons and their effects in production (Milne et al., 1998) as well as a lack of understanding of reaction kinetics in gasification (Dupont et al., 2007). Despite these hurdles, gasification remains a bright focal point of research, understanding and local application (Westmoreland and Harrison, 1976).

2.1.3 Types of Gasifiers

Gasification occurs at high temperatures and in the presence of oxygen or steam which requires well engineered reactors to withstand the intense heat and pressure. The major objective of gasification is to produce a rich syngas for subsequent processes. With this in mind, McKendry (2002) explains that three fundamental gasifiers exist today: fixed bed, fluidized bed and entrained flow. Each category has different strengths and weaknesses in terms of qualities of gasification. The three main gasifiers are detailed in the following paragraphs.

Fixed bed gasifiers are separated into updraft and downdraft reactors. These subtypes are sometimes called co-current and countercurrent due to the direction of the entraining gas relative to the feed stock. In both types, the feed is typically introduced to

the system at the top of the vessel and reacts with hot air while traversing the reactor. The remaining ash accumulates at the bottom while the syngas continues to the next process.

Updraft gasifiers have hot air entering near the bottom of the reactor, which reacts with and partially suspends the feedstock as it travels upwards. Pyrolysis and combustion occur near the bottom, which implies that the temperature of the syngas is relatively low and has a larger composition of tar as it exits the reactor (Belgiorno et al., 2003). Air enters downdraft gasifiers near the middle of the vessel and flows with the falling particles.

The downdraft type allows the feed to be gradually heated until pyrolysis and allows the syngas to leave after flowing through the hot zone, partially cracking the tars. Downdraft gasifiers have a lower tar content and higher energy efficiency due to the syngas leaving at a higher temperature than updraft gasifiers. However, they are also higher in particulate matter due to the proximity of ash to the exit (McKendry, 2002).

Fluidized bed gasifiers (FBG) are designed to overcome some of the shortcomings of fixed bed gasifiers. Fluidization involves a bed of small granular material becoming fluid-like from contact of an upward flowing air or steam (Collot, 2006). Fluidized beds operate at a low flow rate (1-6 feet per second) and a lower temperature (1650°F) than a typical fixed bed (2200°F). The bed of well-mixed particles increases energy efficiency, eliminates temperature zones because of a relatively isothermal bed and ensures intimate mixing between the feed and reacting gas. FBGs also produce lower tar content from the presence of the bed material but also produce a higher amount of particulates than fixed beds. Operating costs are normally higher than

fixed beds because of a large pressure drop across the bed material and distributor plate (Warnecke, 2000).

Entrained flow gasifiers operate at a higher temperature (2200-2900°F) and react at high speed, resulting in a short residence time. They differ from fixed bed and fluidized bed gasifiers by having a burner to produce a stable flame for gasification reactions. Due to the extremely high temperature, the syngas must be cooled before cleaning. The syngas can be cooled by two methods: radiant syngas cooler or quenching the gas with water. Entrained flow gasifiers require the feed to be pulverized (high surface area for reaction kinetics) and the oxidant to feed ratio to be closely monitored (Collot, 2006). Slag produced by the gasifier can penetrate the reactor refractory, creating cracks and eventually leading to material loss. Maniatis (2001) claims that the market attractiveness for entrained flow biomass gasifiers is low due to the requirement of small particle sizes in the feedstock and that the technology is still in the early stages of development.

2.2 Applications of Gasification for Biomass

The use of biomass in gasification is attractive because it is a renewable fuel source. Biomass is available in several forms such as wood, husks and grassy foliage and readily accessible in most populated locations. Renewable energy sources are less likely to pollute the environment and surrounding inhabitants than conventional fossil fuels and are probable sources for replacing petroleum based fuels in several industrial applications (Cummer and Brown, 2002). Some industries are equipped for adapting biomass and have already performed tests in co-firing coal or natural gas with biomass. These tests

reported an increase in gas production and a decrease in char and tar conversion due to the higher volatile compounds found within biomass (Kumabe et al., 2007).

Woody biomass remains the most reliable and appealing source for technology and future use. Gasification necessitates a clean biomass feedstock, which requires time and investment for recovery from natural sources and must also be shared with other markets (i.e., logging, construction, etc.). Industrial wood wastes are attractive because they have already been collected and harvested but are rarely free from chemicals. The strict requirement of a clean fuel has created pretreatment operations that include management of water content, size and storage (Maniatis, 2001).

Though biomass is appealing for reducing dependence on traditional fuels and pollution, it is also capable of producing a syngas which can be used for creating chemicals. The conversion of syngas into chemicals involves catalytic reactions such as Fischer-Tropsch synthesis. The resulting chemicals are, in general, biofuels which generate low amounts of greenhouse gases during energy production or are constituents of other important industrial chemicals (Huber et al., 2006).

2.3 Sulfur Considerations during Gasification

Among the elements that comprise biomass, sulfur is typically one of five of the most abundant (Knudsen et al., 2004). Though sulfur is in significantly smaller concentrations than the largest components, which are carbon, oxygen, hydrogen and nitrogen, its presence cannot be neglected. In commercial applications, impurities can cause serious damage to both equipment and personnel unless they are properly evaluated

and assessed (Gustin, 2002). The major chemical reactions that involve elemental sulfur or a sulfur-containing molecule can be seen in reactions (5)-(8) (Benson, 1977):

$$S + H_2 = 2H_2S \quad (5)$$

$$S + 2H_2O = SO_2 + 2H_2 \quad (6)$$

$$H_2O + CS = COS + H_2 \quad (7)$$

$$CH_4 + H_2S = CH_3SH + H_2 \quad (8)$$

These compounds do not comprise all sulfur compounds but represent the most common species found during combustion and gasification processes. The different types of sulfur species can be seen in the subsequent sections that qualitatively define the classification of sulfur species.

2.3.1 Estimates of Sulfur Compounds

The endothermic conversion involved in biomass gasification results in a syngas and is comprised of several individual gases and elements. The product gas is difficult to predict and control due to the presence of contaminants in biomass. The three major problems are high-molecular weight tars, sulfur and nitrogen, which result in a large array of chemicals and are the focus of subsequent downstream processing (Gangwal et al., 2001). Tar is the most undesirable component but lies outside the focus of this report, which focuses on sulfuric compounds. Sulfur exists in biomass but only in trace

amounts. Osada et al. (2007) stated that biomass may contain as much as 0.5% of sulfur by weight.

Cui et al. (2010) determined that the major sulfuric compounds found in the product gas are hydrogen sulfide (H_2S), carbonyl sulfide (COS) and thiophene (C_4H_4S) in a fluidized bed involving biomass steam gasification. Two other sulfuric compounds, benzothiophene and an unidentified compound, were also discovered in the tar and liquid product in their study. Hydrogen sulfide was found to be in the highest concentration at 93 ppmv, while the other sulfur gases were less than 3 ppmv. Koningen and Sjostrom (1998) also estimate that the average amount of hydrogen sulfide after biomass gasification is approximately 100 ppmv.

2.3.2 Reaction Theory of Sulfuric Compounds

The fundamental elements involved with gasification reactions are hydrogen (H), carbon (C), oxygen (O), sulfur (S), nitrogen (N) and perhaps a few other alkali metals in trace amounts. Benson (1977) laid the foundation of thermo chemistry involving sulfur-containing compounds. The heats of formations involving sulfur and the aforementioned elements can be seen in Table 1. However, some of these structures are more stable than others and leaves only a handful of possible byproducts

Reactions tend to move towards products that are more stable, which are indicated by a negative sign in Table 1. However, the addition of superheated steam adds energy to the reactor, which also allows small endothermic species to be considered. For this review, probable endothermic species are defined as those with a heat of formation of less than ten kcal per mol. After review, 28 sulfur-containing species fit these criteria.

Table 1. Heats of formations of divalent sulfuric compounds at 77°F (adapted from Benson, 1977).

Compound	ΔH_f° kcal/mol	S° cal/mol K	Compound	ΔH_f° kcal/mol	S° cal/mol K
S	66.3	40.1	CH_3S	34.2±1.5	57.6
S_2	30.7	54.5	CH_3SH	-5.4	61.0
c-S_3	32.5±1	63±1.5	CH_2=CHSH	21.0±2	67±1
c-S_4	31±2	72±2	CH_3SCH_3	-8.9	68.3
c-S_6	24.5	84.9	C_2H_5SH	-11.0	70.8
c-S_8	24.5	103.0	C_6H_5S	56.8±1.5	76.5
SH	35±1	46.7	C_6H_5SH	26.7	80.5
H_2S	-4.9	49.2	c-CH_2CH_2S	19.7	61.0
HS_2	22.1±1	61.4	$C_6H_5CH_2SH$	22.9	91.0
H_2S_2	3.8	62.3	$(C_6H_5)_2S$	55.3	
HS_3	25.3±1	74.6	$CH_2(SH)_2$	8±2	
H_2S_3	7.4	75.7	CH_3S_2	17.3±1	
H_2S_4	10.6	89.1	CH_3SSCH_3	-5.8	80.5
SO	1.2	53.0	$C_6H_5SSC_6H_5$	58.4	
SOH	5±4	57±1	CH_3SSS	20.5±1	
$S(OH)_2$	-67±4	70±1	$CH_3S_4CH_3$	0.4±1	
SF	3±2	53.8	CH_3COSH	-43±1	74.9
SF_2	-71±3	61.6	HCOSH	-30±1	
SCl	36.5±2	57.3	$(CH_3O)_2S$	-59±5	
SCl_2	-4.7	67.2	CH_3SCl	-6.8±1.5	
SBr_2	5±4		CH_3SSCl	-5.1±1.5	
FSSF	-80±10	70.3	C_6H_5SCl	25.3±1.5	
S_2Cl_2	-4.7	76.4	$C_6H_5S_2Cl$	27±1.5	
S_2Br_2	9		$(NH_2)_2C$=S	-6.0	72.4
SN	68±5	53.1	HNC=S	30.0	59.2
SC	67±6	50.3	CH_3NC=S	31.3	69.3
CS_2	28.0	56.8	CH_3SCN	38.3	69±1
CSO	-33.1	55.3	$((C_2H_5)_2NS)_2$	-16.5±1.5	
CH_2=S	24.3	56±1	$(CNS)_2$	82.3	

This list can be shortened by assuming that sulfur and other alkali metals exist in trace amounts within biomass and have a small chance of being present within the same molecule (Dupont et al., 2007); a single alkali metal atom is considered possible for any given molecule. This narrows the list from Table 1 down to 12 molecules that are favorable during reactions. The list can be reduced further by making the assumption that methyl groups are not a common result during high temperature gasification; the list contains seven core compounds that closely resemble the list compiled by Cui et al. (2010). Probable sulfuric containing compounds include: (H_2S), (COS), (SO), (SOH), ($S(OH_2)$), (C_2H_5SH) and (HCOSH). It is important to note that all possible divalent molecules containing sulfur are present within Table 1, but leaves out common hexavalent products like thiophene (C_4H_4S) and sulfur dioxide (SO_2). The valence refers to the number of bonds that a sulfur atom can form: two, four or six bonds.

Knudsen et al. (2004) affirm that sulfur in biomass is present in a relatively equal share of organic sulfur and inorganic sulfate. The presence of elemental sulfur typically gives hydrogen sulfide while inorganic sulfate leads to higher order molecules. According to Evans and Wagman (1952), sulfur is most likely to be divalent and hexavalent in naturally occurring mixtures. They also state that sulfur dioxide and sulfur trioxide are stable compounds after exothermic reactions, have heats of formations between -100 and -70 kcal/mol and result in a high concentration of sulfur dioxide at elevated temperatures. The presence of water as the major source of oxygen helps to limit the formation of sulfur dioxide and creates a rich syngas product stream.

2.3.3 Sulfur Release during Pyrolysis

Garcia-Labiano et al. (1995) explain that the distribution of sulfur in char, gas and tars during pyrolysis is dependent upon the reactor conditions. The reactor type, heating rate, peak temperature and residence time affect the type and amount of sulfuric compounds located in the ensuing products. Though their efforts were focused on pyrolysis of coal, which contains a higher percentage of sulfur, they found similar sulfuric compounds as reported by Cui et al. (2010), including hydrogen sulfide, carbonyl sulfide and carbon disulfide with hydrogen sulfide being the most abundant.

Temperature has a significant influence on product distribution. At lower heating rates, Yaman (2004) concluded that carbonization was favored and reduced the yield of liquid fuels. He further states that gases became the main products at temperatures higher than 1300°F. Knudsen et al. (2004) reported that sulfur release into the gas phase was negligible at lower temperatures and remained within the bed. Sulfur release increased with rising temperature and at 1750°F, approximately 85% of the total sulfur was released. Expectations indicate that the high gas conversion achieved at elevated temperatures and favored in gasification can be accompanied by increasing sulfur amounts in the syngas.

2.4 Minimization of Sulfur Compounds

Some of the undesirable effects of sulfur include degradation of catalysts and equipment, and an associated reduction in desired product production. Sulfur compounds can be especially harmful to personnel and the environment. It is, therefore, a good idea to reduce the concentration of produced sulfur-containing gases to minimize the expected

consequences. Ideas for containment include post-processing cleanup, selection of biomass and catalysts, and operating conditions which are explained in further detail in the succeeding sections.

2.4.1 Catalyst Degradation

Biomass gasification produces a significant amount of tar and sulfuric compounds that degrade catalysts and inhibit liquid fuel production (Rapagna et al., 1998). In order to produce liquid fuels and remove tars, catalysts are employed to lower the activation energy and crack tars into constituent components. The presence of sulfur decreases a catalyst's ability to work effectively by binding to the catalyst, which must either be cleaned or replaced to resume production (Bain et al., 2005). Osada et al. (2007) report that sulfur negatively affected gas conversion during gasification to 75-93% of normal operating conditions and gives convincing evidence that the production of gas was severely hindered to 20% by increasing the concentration of sulfur by four times the normal amount. They further argue that catalytic degradation is evident from their data and is attributed to the reduction of active sites on the catalyst. Conversion can be maintained by installing sulfur cleaning processes upstream of the catalyst system.

2.4.2 Gasification Management in Reducing Catalytic Poisons

Catalysts are proving to be useful in helping to reduce tar production but can be easily poisoned and rendered ineffective if not maintained properly. Defense against catalytic poisons is achieved by zero contaminant production or by reducing their effects, which can be achieved by clever manipulation of gasification settings. Osada et al.

(2007) stated that the effects of sulfur on catalytic active sites can be reduced by having a high water concentration. Catalysts have a significantly higher surface area located in the pores than on the catalyst surface. The increase in water molecules reduces the ability of sulfuric containing molecules to reach the active sites located within the pores of the catalyst by acting as obstructions. The effect of high water density on the cracking of tar is not mentioned.

Another method of reducing the effects of sulfur as a catalytic poison is to replace the catalysts with ones more tolerant of sulfur. Wang et al. (1997) described a novel catalyst that is less susceptible to sulfur poisoning and which is a mixture of rare earth metals. Current catalysts are typically comprised of NiO, Zr_2O_3 and a few other rare earth metals such as cesium and silicon. These newer types of rare earth metals can increase the life of the catalyst from only a few hours to several days. Tomishige et al. (2004) also reported favorable results when a newly developed catalyst was employed that was made from a combination of $Rh/CeO_2/SiO_2$. They also suggest that traces of sulfur on the catalysts can be removed by oxidation or reduction within the fluidized bed reactor.

Alternative ideas include particle sizing, leaching and other downstream processes that are capable of removing contaminants. Cummer and Brown (2002) stated that these additional steps were effective in reducing sulfur by 70%. These applications, however, have limited uses when syngas or Fischer-Tropsch fuels are the desired outcome.

CHAPTER 3

EXPERIMENTAL

3.1 Introduction

Although the University of Utah operates a pilot-scale fluidized bed biomass gasifier, there is value in having a smaller, bench-scale system. Advantages include: a more manageable size reactor for a single researcher, a more responsive system for various test settings and conditions, challenges operating the pilot scale fluidized bed and a significant decrease in utility consumption and costs. These factors were considered and ultimately led to the decision that a 4-inch fluidized bed would be suitable for this project even though significant time and effort would be needed for construction and development of the reactor. With the dimensions of the pilot scale design in mind, a four-inch apparatus was constructed with comparable features to produce similar results. However, a few modifications relating to analysis were needed for practicality.

The following subsections show how the system was originally designed and how, through the process of experimentation and reconstruction, the system has progressed to its present state and current layout. The design and operation of the system is described in detail for review as well as observations regarding operation of the system.

3.2 System Description

The 4-inch fluidized bed gasifier consists of a long tubular reactor, a boiler, a steam preheater, bed heaters, feeding system, a particle capture system, analytical instruments and a control system. Some of these pieces have undergone several revisions in order for the apparatus to work successfully. The fabrication, design and the progression of the experimental bench scale gasifier have proved to be the most difficult and time consuming portions of the project. In some cases, development of a new system or technology consumes the most resources as information regarding the subject may be sparse or completely undocumented. For these reasons, details regarding the evolution of the reactor and subsystems are given in sufficient detail such that future work may be continued. The following sections describe the development of the critical areas of the reactor.

3.2.1 Reactor

The reactor is comprised of three sections: a plenum chamber, the fluidized bed and the feed section. The three sections are held together by stainless steel flanges, nuts and bolts and carbon gaskets. These sections are seen in Figure 3 for analysis. The reactor began with a 4-inch diameter pipe made of 321 stainless steel, which was selected because of its good corrosion resistance at high temperatures and high heat conduction. These attributes eliminated the need for a refractory shell. Four inches was determined to be the appropriate reactor diameter because it is the largest diameter that can provide enough surface area from the reactor walls to heat the bed material. Reactors with a larger diameter require bed heaters within the reactor to supply the necessary heat.

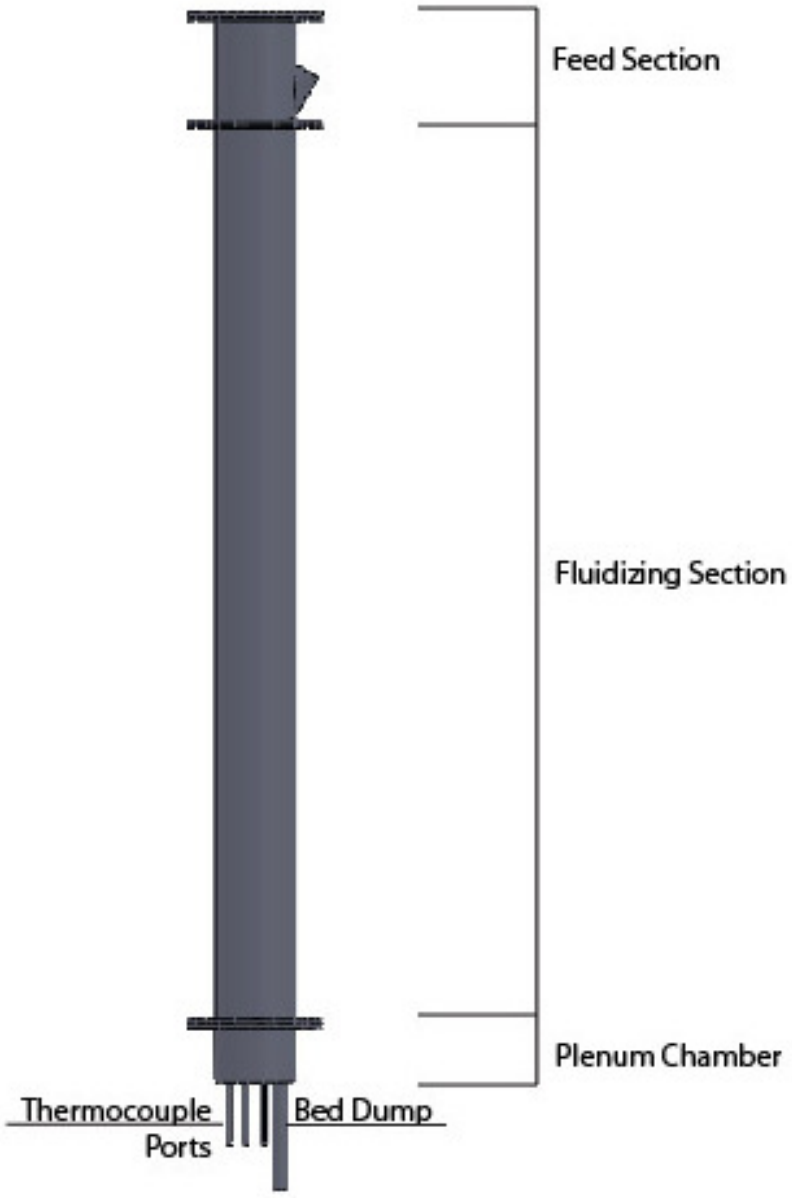

Figure 3. Diagram showing the three main sections of the reactor.

Four feet was selected as the height because it provides a residence time of approximately 17 seconds. The overall design of the reactor is effective. The simple design and no moving parts allow the system to be maintained and cleaned easily. The bracketing system that hangs the reactor from the top of the fluidizing section allows the feed or plenum sections to be removed easily and separately. This design also allows the reactor to expand towards the ground leaving the feed section in a stationary position despite the reactor growth during heating.

3.2.2 Plenum

Steam is introduced into the bed of material through the plenum and dispersed evenly across seven bubble caps arranged in a concentric circle. The plenum itself is a sealed 4-inch chamber constructed from 321 stainless steel with five 0.25-inch tubes that run through to allow thermocouples access to the bed and a one-inch pipe that allows the bed to be dumped. This part of the reactor is difficult to explain because of its complex nature. Figure 4 shows a diagram of the plenum and the respective dimensions. Thermocouples were inserted through the tubing to record bed temperatures at 1, 3, 9, 12 and 15 inches.

The bubble caps are constructed of 316 stainless steel rods that had been cut, drilled, welded and tapped so that it could be threaded into the plenum for easy installation and disassembly and can be seen in Figure 5. The bubble caps were a concern early on because they have allowed weeping of the bed particles into the plenum. On a few occasions, the plenum became full of bed particles which produces a larger pressure drop across the distributor and gives an opportunity for steam to condense

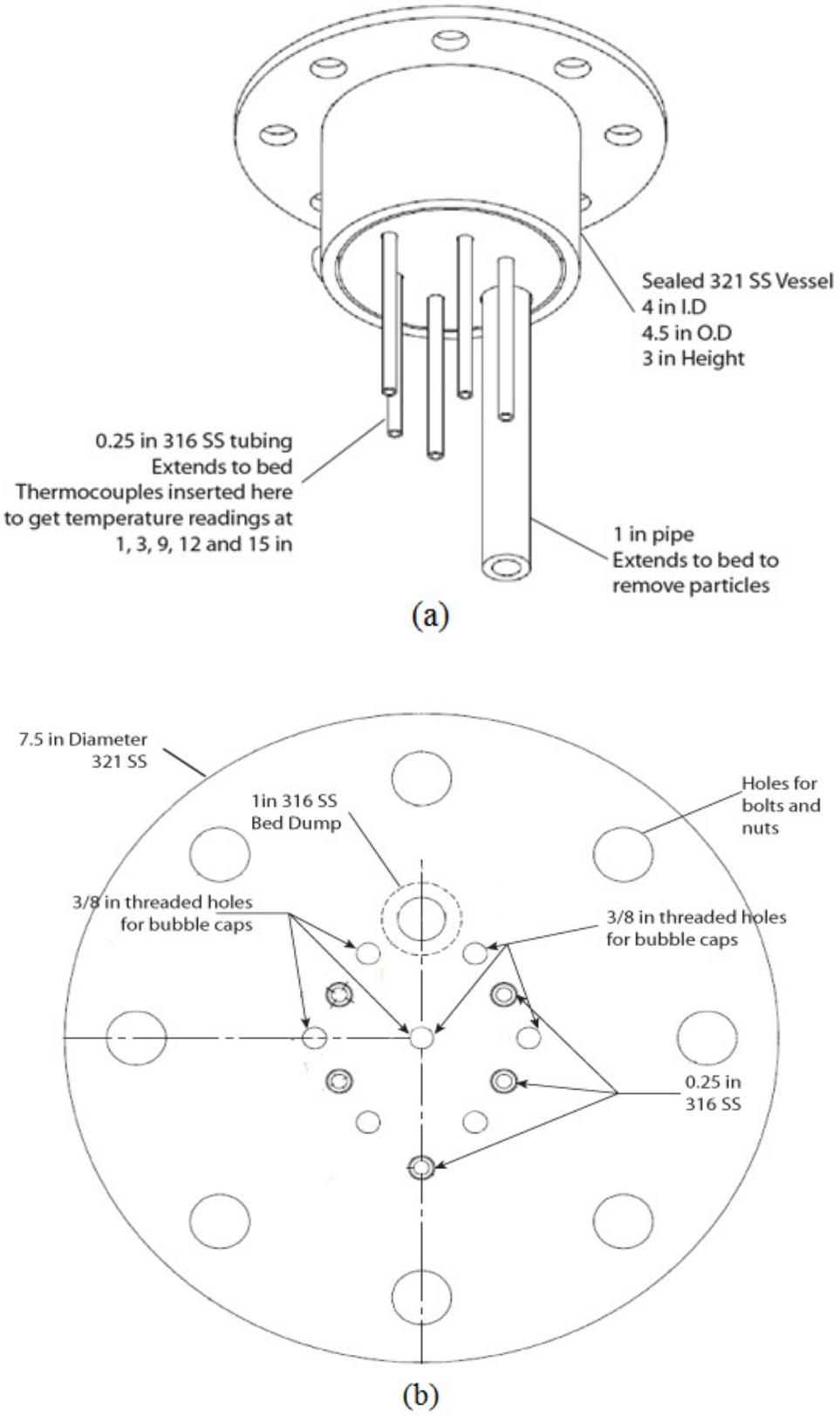

Figure 4. Diagrams of the plenum. (a) bottom view (b)Top view

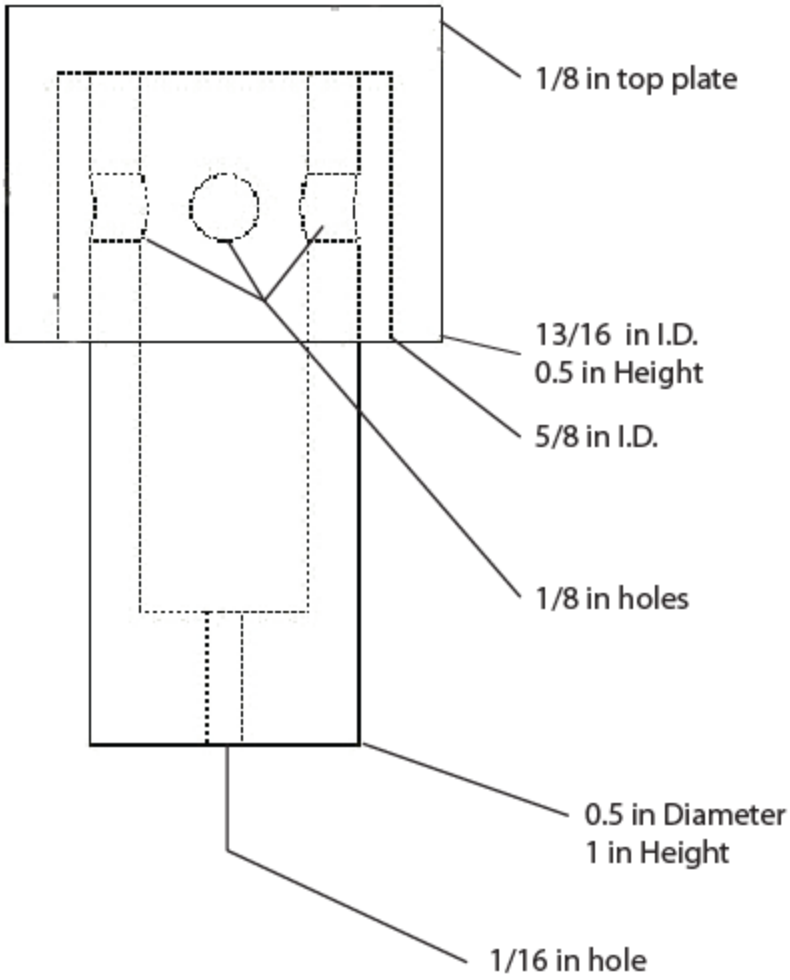

Figure 5. Schematic of the bubble cap assembly and dimensions.

before introduced into the bed. These problems have been minimized by keeping the plenum regularly cleaned and holding a steady flow of air, nitrogen or steam through all stages of experiments. Weeping can be eliminated by replacing the bubble caps with ones that have smaller holes or redesigning how steam is introduced from the plenum into the reactor.

3.2.3 Feed Section

The feed section has been separated from the fluidizing section, which is surrounded by heaters, so that the feeder and biomass do not receive direct heating and combust before the biomass enters the reactor. The feed section consists of another four-inch pipe that is 6 inches tall with a 1-inch coupling placed at a 60 degree angle for the injection of biomass. The reactor is capped with a blind flange with a 1-inch coupling inserted in the middle for the syngas outlet. A major problem of the reactor early on was the feed section plugging, caused by a necked-down section of 1.5 inches to a one-inch diameter pipe connected to the coupling. Biomass simply could not traverse down a 1-inch pipe and then cross through the coupling and into the reactor, plugging quickly and often. A purge line was placed right above the insertion point of biomass from the feeder to blow the fuel into the reactor and prevent plugging. This, however, did not solve the matter because ash would collect onto the coupling and feed section to which the biomass would stick and eventually plug.

The 1-inch coupling ultimately needed to be capped and the top flange redesigned to allow the biomass to simply drop into the reactor. The top flange was reconstructed to allow for a larger 2-inch diameter pipe that would be more difficult to plug. The piping

that introduced the feed to the reactor was a solid welded piece except for a single union which had been smoothed, removing all rough surfaces for ash to collect. A better purge was installed that injected nitrogen at the entrance of the piping and which blew the biomass particles more forcefully into the bed. A dividing plate was also welded to the top flange to break the feed section into two parts: an entrance for the feed and an exit for the syngas. The current setup for feed insertion can be seen in Figure 6. This helped prevent the biomass particles from being entrained by the syngas and swept away before they had time to react. This reconstruction of the feed section has prevented further plugging.

3.3 History of System Development

The original layout of the utilities involved steam being produced from the same boiler used for the pilot scale gasifier and, through a series of valves, sent to a flow meter, then the preheater and finally the plenum. Air was introduced into the steam line before the flow meter so that the system could be started on air. Starting the system on air allowed the system to be heated sufficiently to prevent the condensation of steam into a cold reactor. Cold nitrogen was introduced into the same line just before the plenum chamber, serving as an additional fluidization gas that could be used without combusting the biomass in the reactor, assuming the reactor is hot.

A few problems arose from this setup; mainly an inconsistent supply of steam and the introduction of cold nitrogen into a line with superheated steam caused the formation of condensate within the plenum, lowered the bed temperature and allowed more weeping of bed particles into the plenum. The steam supply challenges were solved

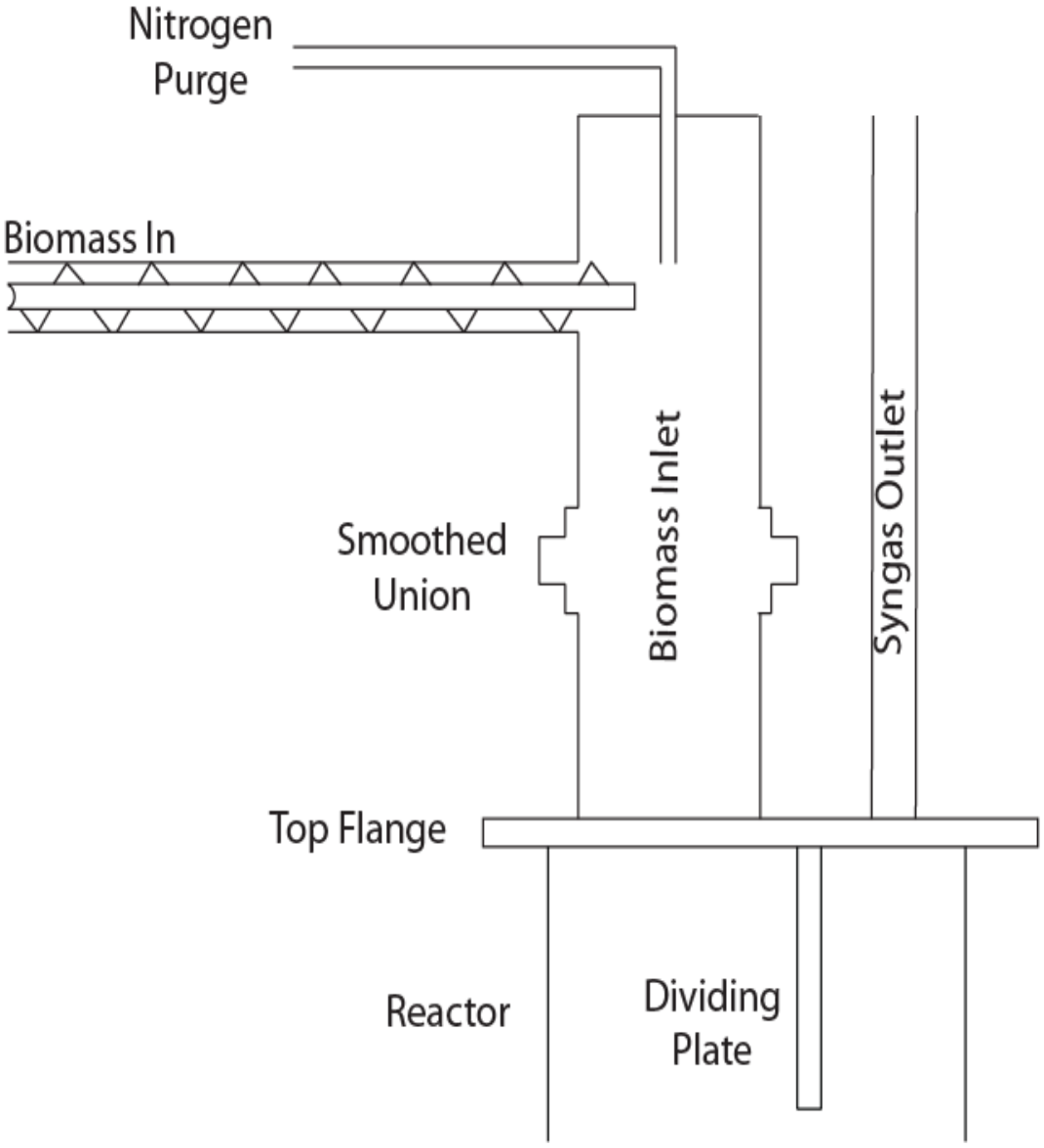

Figure 6. The current setup for biomass insertion into the fluidized bed reactor.

by observing the cyclic nature of the boiler. The boiler was designed to feed the pilot scale gasifier at a consistent rate and produced much more steam than was necessary for the small bench scale gasifier. This caused the boiler to turn and produce steam until 90 psig was reached in the boiler and then turn off, once the pressure dipped lowered, it would turn on again. This resulted in an inconsistent amount of steam being sent to the flow meter. A pressure regulator was placed on the steam line from the boiler to provide a consistent flow rate and stabilized the system.

The problem with the supply of cold nitrogen was finally corrected by introducing nitrogen before the preheater and wrapping the inlet with a variable control silicone heat tape. The heat tape was wrapped around the steam line until up to the preheater. This correction eliminated any steam condensation and served as an additional inlet of heat, relieving some stress off of the preheater and increasing its output by roughly 70°F. Additionally, a three-way-valve was added to the steam line after the flow meter to remove any condensed steam that may have accumulated from heat loss to the flow meter.

As described in the literature review, during gasification a noticeable amount of tars and ash are produced which can cause problems with downstream processes. This was viewed first-hand as tars began to condense on the line removing the syngas from the reactor and as ash began to adhere to the tars until the line or other downstream instruments finally plugged and a large pressure in the reactor was produced. This was easily remedied by increasing the outlet line from 0.5 to 0.75 inches and including an ample amount of heat trace to the line. During experiments, this line was kept above 600°F and verified by a thermocouple. A filter was included just after an impinger (water

quench) to prevent ash and other particulate matter from traveling downstream and ruining subsequent instruments, namely the dry gas meter and pressure gauges. The system performed better if the filters, gauges and meters were inspected and cleaned after each experimental run.

The layout of the system was also reorganized to allow a single individual to be able to watch all gauges, control system, flow meters and the feeder output. Also, a panel was created to accommodate all the flow meters in a general location. This restructuring has improved the time management of those involved with testing. With these improvements to the utilities and reactor in place, the system began to perform consistently and similarly to the pilot scale fluidized bed gasifier. However, even with these upgrades, ash and other particulates can still begin to accumulate and should be cleaned out regularly.

Despite the amount of work done, additional upgrades could be performed on the reactor and utilities to yield better results. Some of the improvements include: adding a cooling system to the feeder and vertical feeding tube, the addition of more calibration gases for analytical purposes, more instruments that are integrated into the control system and a smaller and more efficient impinger. These additions would give better accuracy and precision to the apparatus as well as increased operational stability and control.

3.4 Sampling System

The main analytical instrument is a Varian CP-4900 micro gas chromatograph. One liter per minute was pulled from the reactor outlet containing the syngas and sent for

analysis. The gas chromatograph used 60 mL per minute of the sample gas for the composition testing.

The sampling system also required a few revisions for a correct sample analysis. Initially, the sampling port was placed after the impinger (water quench) to protect the chromatograph from ash, tars, water vapor and other harmful particulate matter. This approach works fine for analysis on gas species that do not condense or dissolve in the impinger, such as hydrogen, carbon monoxide, carbon dioxide methane, etc. and was used during initial tests and trials of the apparatus until reasonable operating stability was established. However, one of the objectives of this experiment was to determine the concentration and trends regarding species that contain sulfur, which are soluble in water. Therefore, modifications to the sampling system were necessary to allow the impurities to be effectively removed without affecting the gas species and damaging the chromatograph.

Reducing the temperature of the sample stream and removing the particulates, without allowing the steam to condense is necessary before the sample can reach the chromatograph. The solution requires removing the water while still in gas phase. Perma Pure makes a dryer that is capable of performing this task. The dryer resembles an annulus with the inner wall replaced with a permeable membrane. This membrane is made from Nafion®, a Dupont co-polymer that is highly selective due to the inclusion of sulfonic acid groups. These groups are formed into small channels that extend from the interior to the exterior of the surface due to their ionic nature. The sulfonic acid groups are very hydrophilic and readily bind with water in a reversible reaction as water-of-hydration. The water molecules then move through the small channels to the exterior

surface where it is removed by pervaporation. This dryer is capable of selectively removing the water vapor from the sampling stream.

A filter was placed in the sample line before the dryer to prevent particulate matter and ash from reaching the dryer or chromatograph. These additions to the sample line water and ash, but do not consider the tars that form during biomass gasification, or temperature control. Tars are a mix of high molecular weight aromatic hydrocarbons that are sticky at ambient temperatures. Since they are a mixture, it is nearly impossible to selectively remove them from the sample stream, but is more typical to collect them as they condense. The wide range of components found in tar begins to condense below 600°F. The tars in the sample stream need to be cooled and collected without allowing the water vapor to condense. The dryer must operate above the dew point of the sample stream in order to remove water effectively. If the water vapor condenses, the water-soluble gas components will also condense. The situation can be resolved by maintaining the filter at 250°F, thus condensing the tars and collecting particulate matter while still allowing the wet gas to continue downstream to the dryer.

This configuration removed the tars and ash, but only a portion of the water vapor was removed within the dryer. The remainder of the water condensed in the line outside of the dryer and created a small pool, only allowing insoluble gas species to pass. The pressure inside the dryer was identified as the problem. The dryer requires a wet gas sample to travel down the center of the annulus, while a dry purge gas runs countercurrent around the outside. This allows the moisture to pass through the Nafion membrane as long as the pressure of the wet gas is higher than that of the purge gas. The heated filter created a large pressure drop, requiring a pump to pull the sample through

the filter. The pump was initially located before the chromatograph, pulling the sample through both the filter and dryer causing a vacuum in the center annulus. The pump was then exchanged for a different one with a heated head which was placed before the dryer, pushing the sample through. A heated head on the pump was necessary to prevent the water from condensing before reaching the dryer.

Finally, heat trace, thermocouples, pressure gauges and needle valves were installed to ensure that the temperature was maintained at 250°F and a positive pressure remained in the dryer. The water vapor is removed by pervaporation into a dry nitrogen purge flowing at three liters per minute. Pressure is maintained inside the dryer by use of the pressure gauge and throttling valve to ensure that the syngas pressure remains above the pressure of the nitrogen purge. Finally, the flow rate of the syngas is measured through a rotameter before traveling to the gas chromatograph for analysis. After these revisions, the chromatograph began to yield a more complete picture of gases produced from the reactor. A schematic of the final arrangement of the sampling line can be seen in Figure 7.

3.4.1 Gas Analyzer

The syngas produced during each experiment is sent to a gas chromatograph after the water vapor, tars and particulate matter have been removed. For these experiments, a Varian CP-4900 micro gas chromatograph with four independent operating columns was selected because of its quick response time and portability. The analyzer was used in conjunction with Galaxie software, which assisted in controlling the gas chromatograph and preserved the data for analysis after the experiments were completed.

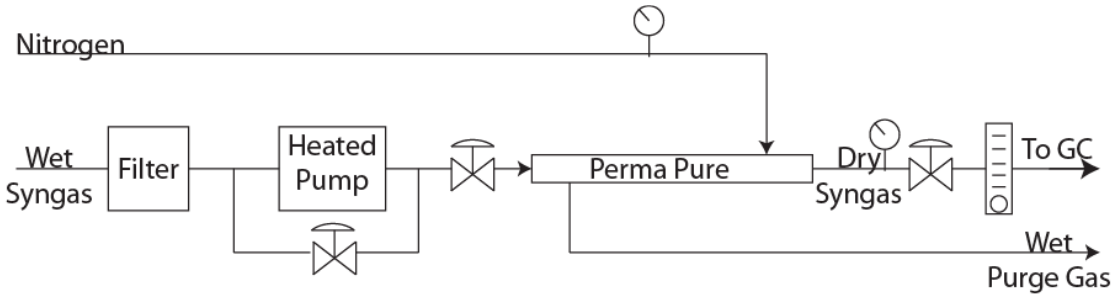

Figure 7. Schematic of the final layout of the sampling system.

Each of the four columns within the gas chromatograph was selected to identify a different range of gaseous components. The first column analyzes the major components that result from gasification, namely: hydrogen, oxygen, nitrogen and carbon monoxide. The second column can detect other common compounds that comprise a significant portion of the syngas and include: methane, carbon dioxide, ethylene and ethane. The second column also includes the major sulfur species produced during gasification: hydrogen sulfide, methyl mercaptan and sulfur dioxide. The third column is used to detect additional hydrocarbons that may be present in small amounts, including propane, propylene, acetylene and butane. The final column recognizes hydrocarbons that may exist in trace amounts, specifically pentane and hexane. With each of the columns designated to identify a different set of compounds, a broad distribution of gases and their respective compositions can be obtained through experimental procedure.

3.5 Equipment Configuration

A simple diagram of the overall system and gas flow can be seen in Figure 8. A table of all equipment and their dimensions used in the experimental process can be seen in Table 2. The apparatus begins with steam entering the system and flowing into a pressure regulator set for 30 psig. This provides a consistent supply of steam from a boiler that is inconsistent at providing steam at a small scale. The flow rate of steam is controlled by a rotameter designed for steam at 50 psig. The discrepancy between the different pressures, 30 and 50 psig, is corrected by accounting for the change in density. The rotameter has a range of 0.5 to 5 lbs per hour of steam. The steam then flows through a three-way valve allowing the steam and condensate that forms to leave the

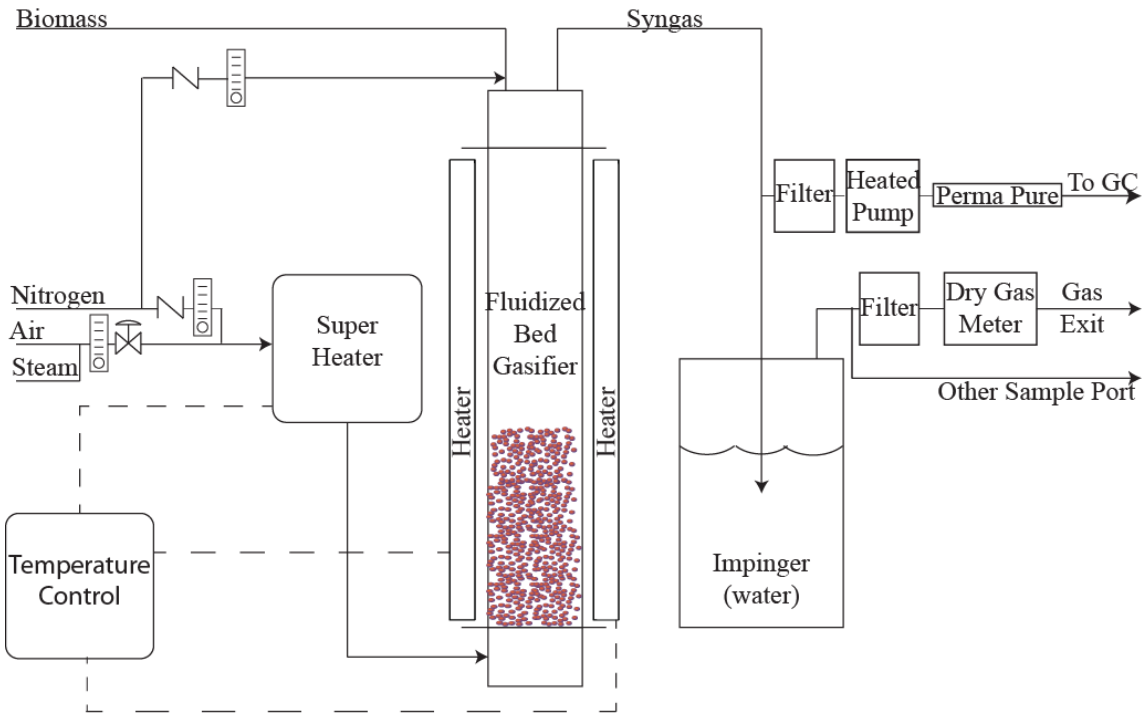

Figure 8. Schematic of the overall system.

Table 2. List of all equipment used in the apparatus and their respective dimensions.

Equipment Description	Type/ Material	Diam.	Equipment Description	Type/ Material	Diam.
Steam Generation			Feed Section	321 SS	
Pressure Regulator	Hoffman Type 754		Height		6 in
Tubing	316 SS	0.25 in	Inside Diam.		4 in
Flow Meter	Krohne DK32		Outside Diam.		4.5 in
Flow Rate		3.5 lb/hr	Feed Pipe Length	316 SS	9 in
Steam Preheater			Feed Pipe Diam.	316 SS	2 in
Coil Length	316 SS	7 ft	Feeder		
Coil Diameter	316 SS	0.5 in	K Tron	Volumetric Feeder	
Heat Trace	HTS Amptek	10 ft	Feed Rate		1-2 lb/hr
Thermocouple	Type K	0.125 in	Feed Section Outlet		
Plenum	321 SS		Tubing Diameter	316 SS	0.75 in
Inside Diam.		4 in	Heat Trace Length		20 ft
Outside Diam.		4.5 in	Thermocouple	Type K	
Height		3 in	Impinger	Carbon Steel	
Bubble Caps	316 SS		Height		30 in
Height		1.25 in	Diameter		20 in
Stem Diameter		0.5 in	Water Height		24 in
Center Hole		0.0625 in	Impinger Inlet	316 SS	0.75 in
Side Hole		0.125 in	Impinger Outlet	316 SS	0.5 in
Cap Diameter		0.8125 in	Dry Gas Meter		
Cap Thickness		0.125 in	Dry Gas Meter Outlet	Polyprop	0.5 in
Reactor	321 SS		Sampling System		
Inside Diam.		4 in	Tubing Diameter	316 SS	0.25 in
Outside Diam.		4.5 in	Heated Pump		
Height		50 in	Perma Pure Dryer	MD-110	24 in
Watlow Heaters	120V 3000W		Gas Chromatograph	Varian CP-4900	
Bed Heater Ht.		18 in	Opto 22	Control System	
Watlow Heaters	240V 5000W		Silicon Heat Tape	Brisk Heat 120V	
Heater Height		30 in			

system while the preceding piping and instruments heat up. The remainder of this line is traced with temperature controlled silicone heat tape that serves to elevate the temperature and prevent any condensate from forming before entering the preheater.

The preheater was constructed in house and is comprised of approximately 7 feet of 0.5-inch 316 stainless steel tubing bent into a coil. The tubing is tightly wrapped with high temperature heat trace (Maximum temperature of 1200°F) with a type K thermocouple, located halfway down the coil and attached in between the tubing and heat trace, which serves as feedback to the control system. The coil is wrapped with a thick blanket of fiberglass insulation with a thin sheet of aluminum secured around the outside of the insulation. The apparatus resembles a small cylinder that is capable of raising the temperature of the steam to approximately 1030°F.

The steam continues to the plenum where it expands into a chamber that is 3 inches in height and 4 inches in diameter, exerting an even pressure across the bubble caps above. A pressure gauge is located on this line and indicates the pressure drop across the bubble caps. The bubble caps are constructed of 316 stainless steel rod and are 1.25 inches in height; the bubble caps only extend one inch above the surface of the plenum as 0.25 inches are threaded into the plenum. An 1/16 inch hole is drilled into the center of the stem at the bottom that is 0.25 inches in height, producing the pressure drop. The rest of the stem then expands to 1/8 inch where 1/8 inch holes are drilled orthogonally to intersect the center point. Half of the stem is then covered by a cap that has been welded to the top of the stem.

Once the steam crosses through the bubble caps, it enters the fluidized bed section which contains 4.4 pounds of bed particles. The bed particles are a proprietary spray-

dried aluminum oxide material supplied to the project by ThermoChem Recovery International, Inc. (TRI). The average particle size is approximately 225 microns in diameter once the material has been sifted through a number 50 sieve. The particles have a low bulk density of 1.1 grams per mL which is attributed to their hollow core.

The bed of particles is heated by 4 Watlow ceramic fiber heaters. The heaters are semi cylindrical in shape, which provides an equal distance from the heaters to the surface of the reactor. The two heaters located on the bottom half of the reactor are 18 inches in height and use 120 V to produce 3000 W from each heater and are used to direct the bed directly. The top heaters are 30 inches in height and use 240 V to produce 5000 W from each heater and are stacked on top of the bottom heaters and are mainly used to heat the freeboard. The heaters convey energy by radiation since they are situated 2 inches away from the reactor. Each pair of heaters has a thermocouple attached to the surface of the reactor to provide feedback to the control system. The heaters are capable of heating the bed to 1800°F. However, the bed temperature in this project reaches a maximum of 1350°F.

Additional thermocouples have been placed inside the bed to monitor the temperature. Five thermocouples are located between the bubble caps in a concentric circle and measure the temperatures at 1, 3, 9, 12 and 15 inches above the bubble caps. The first three thermocouples measure the temperature of the bed (assuming the bed is nine inches in depth), while the last thermocouples measure the temperature above the bed or of the particles falling back to the bed. All temperatures are recorded and displayed on the control system.

Biomass is inserted into the bed via a K-tron volumetric feeder. Two small augers push biomass from a hopper, which holds roughly 2 gallons of material, into a vertical 2-inch diameter pipe that was welded to the lid and explained in section 3.2.1. The augers are roughly 1-inch in diameter with quarter-inch grooves that can handle only small biomass sizes. It was necessary to grind the biomass into a smaller size so that it could fit into these grooves. The switch grass was approximately quarter-inch flakes while the pine chips had a range of sizes from 0.1 to1 mm. The feeder has a digital readout which can be manually controlled by setting the feed rate between 0 and 100%. A series of calibration tests were required for each fuel to equate the percentage into a weight. The feeder calibrations can be seen in Appendix A. Tests show that the feeder is capable of inserting from 3.75 to 2.0 lbs per hour depending on the type of biomass and its respective density. The biomass then falls into the reactor where syngas is produced by steam gasification.

The syngas exits the reactor through 0.75-inch stainless steel tubing that is connected to the top flange via a coupling. This length of tubing is wrapped with high temperature heat trace and is kept above 600°F to prevent tars from condensing and plugging the system outlet. Three thermocouples have been placed on this line, two serving as feedback for the control system to the heat trace, while the other simply monitors the temperature of the syngas before exiting into the impinger.

The impinger is constructed from a small 30 gallon, round, sealed steel drum. The drum is 30 inches in height and has a 20-inch outside diameter. The syngas is inserted into the middle of the removable lid through a welded coupling. The opposite end of the coupling is expanded to a 1.5-inch pipe that extends 18 inches into barrel.

Cooling water is brought into the bottom of the barrel through a small port and is allowed to fill the barrel to 24 inches in height, where the water exits, by gravity. The hot syngas enters the barrel through the 1.5-inch pipe and begins to cool by bubbling through the cold water, condensing the tars, lowering the gas temperature and collecting the particulate matter into the water. The gas then exits through 0.5-inch stainless steel tubing, placed slightly off center, connected to the removable lid. The dirty water is removed through a large opening that leads to a drain, the end of which is elevated to prevent syngas from escaping by creating a wall of water, and where samples of the water can be collected for analysis.

After leaving the impinger, the cool syngas enters a small filter that removes any additional particulate matter that may not have been collected in the impinger and then finally exits through a dry gas meter. Any particulate matter that collects in the filter may be examined and measured after the experiment finishes. The dry gas meter does not have a digital readout and must be measured periodically throughout the experiment.

The electrical equipment is controlled and thermocouple temperatures are recorded by Opto22. This is sophisticated control software that allows control and measurement of several instruments by an operator. A case and shelf has been installed on the structure of the apparatus to house all of the controls, signals, computer and monitor. Opto22 is mainly used for controlling the heaters by using a PID feedback control and for measuring and recording additional thermocouple points. The display used by Opto in controlling the heaters can be seen in Figure 9. The software also included an emergency shutdown, PID tuning parameters and graphs showing the temperature profiles of the different heaters and thermocouples.

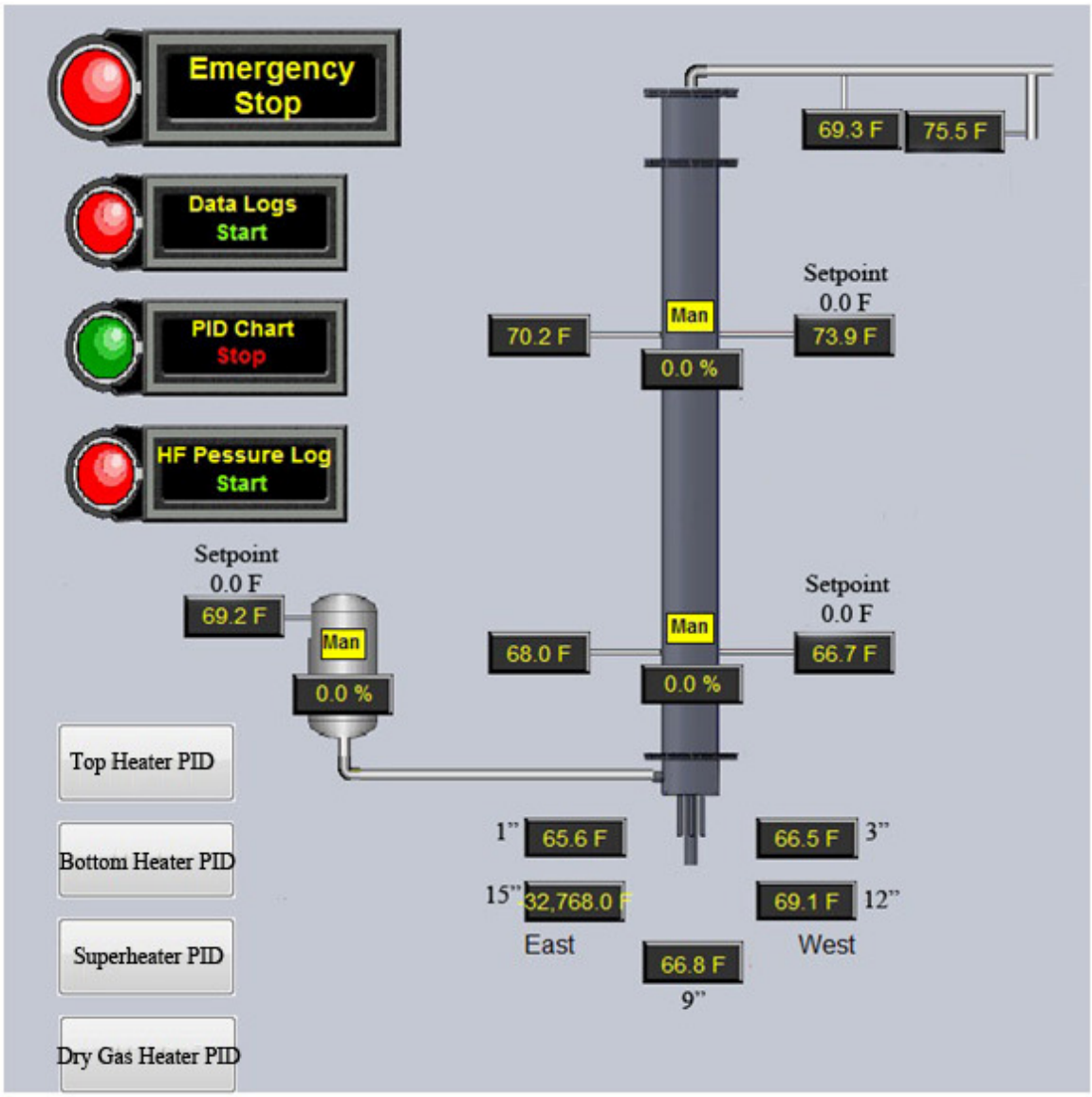

Figure 9. The display used by Opto22, the control system.

The overall layout of the bench scale gasifier has improved over several revisions and now runs effectively. Front and back photographs of the apparatus can be seen in Figures 10 and 11, respectively.

3.6 Operational Procedure

Power to the both 120 V and 240 V is supplied by turning on the switches from panels located near the reactor. The PID tuning charts must be started within the control display as a safety precaution. Air is supplied to the system, while increasing the set point to the bed heaters and preheater by 200°F until the desired bed temperature is met (roughly 1250°F). The heat trace located on the reactor outlet is increased by 100°F until the temperature rises above 600°F. The heated pump and filter for the sampling system are turned on, allowing the sample line to become warm. The silicone heat tape located on the sample line and before the preheater is turned on. Once the reactor, outlet line and sample line reach 1250, 600 and 250°F, respectively, the boiler is turned on and allowed to reach pressure. The entire heating process takes about 2-2.5 hours for the system to come to steady state.

Nitrogen replaces the air as the fluidizing gas while steam preheats the preceding instruments and piping and condensate is removed from the system. The dryer and feeder purges are set to 3 and 8 liters per minute, respectively. Steam is then co-fed into the reactor with the nitrogen; nitrogen flow is slowly decreased and steam increased until steam is the only fluidizing gas and measures 5 lbs per hour. The system is allowed to equilibrate once again, since steam draws more power than air for heating. Once steady state occurs, approximately another hour, the dryer is checked and ensured that no

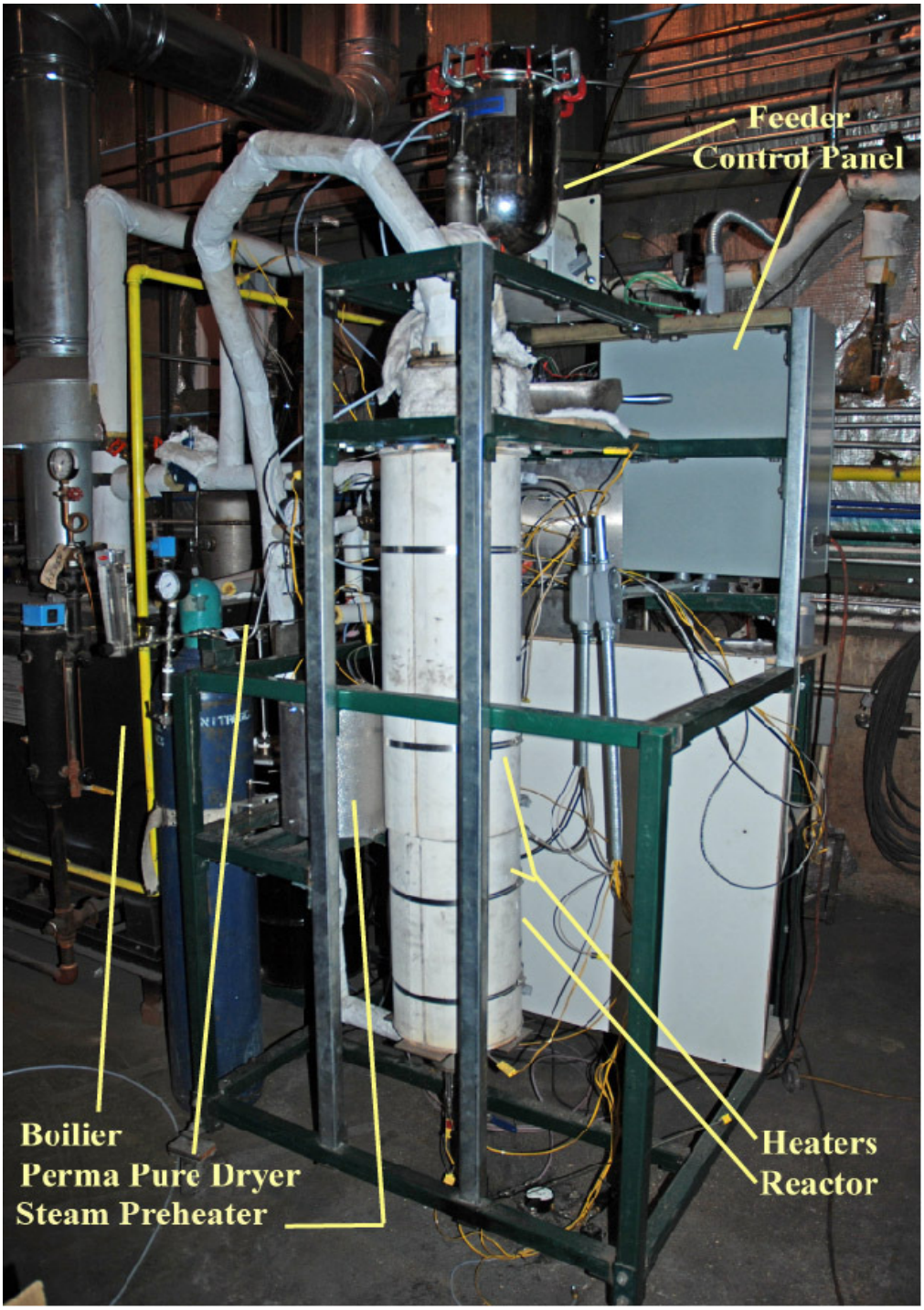

Figure 10. A front view of the reactor, which shows the reactor, heaters, feeder, boiler, Perma Pure dryer and control panel.

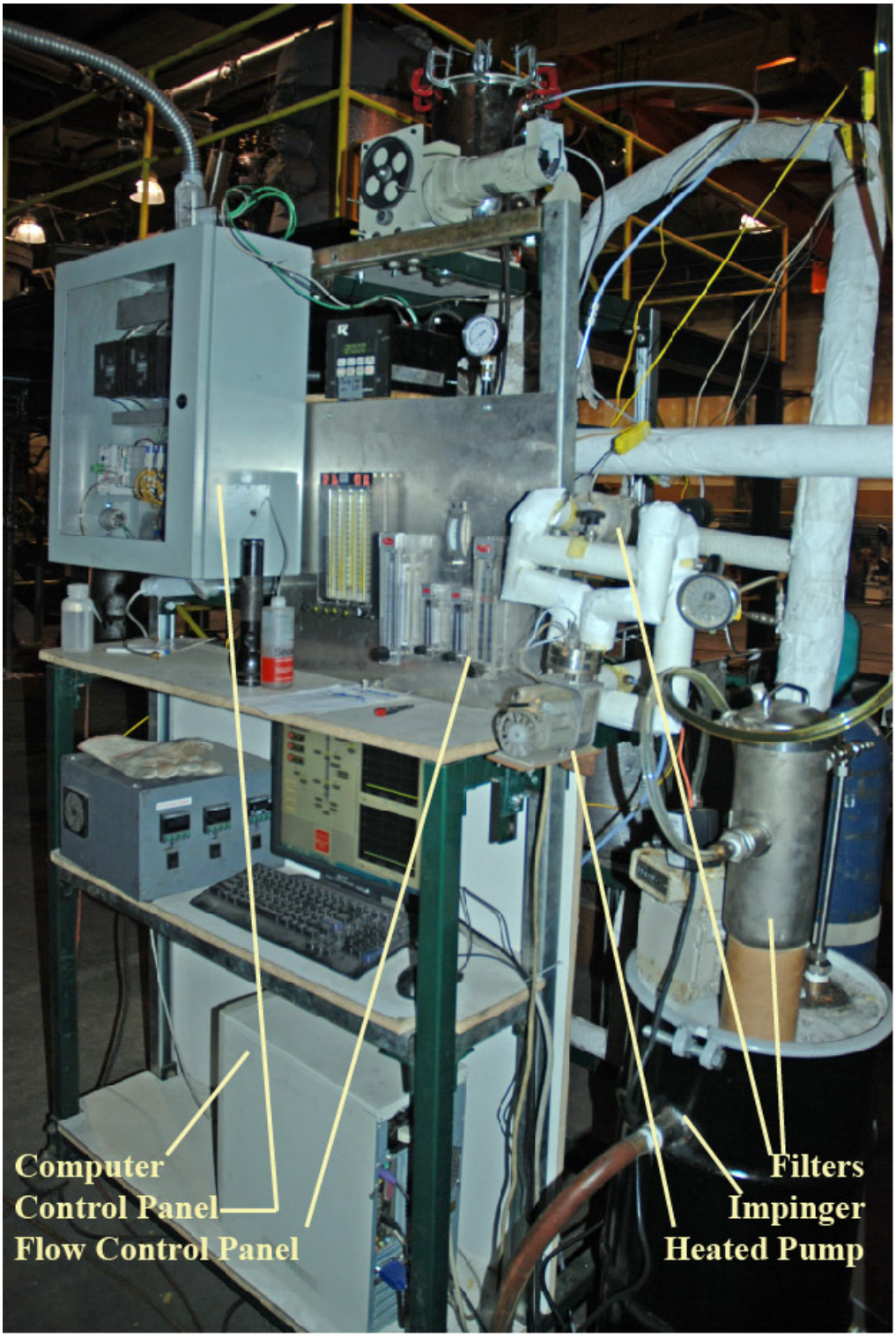

Figure 11. Back view of the apparatus, showing the control panel, computer, impinger, filters, heated pump and flow control panel.

condensate is present. The feeder can then be turned on and the gas chromatograph can be attached and started. The experiment can then run until the hopper on the feeder runs out of material (approximately 4 lbs of material depending on density). It is possible to slump the bed and fill the hopper with more biomass if additional tests are to occur. However, this is not recommended because noxious gases can emerge through the hopper once the lid is removed and poses a risk to the operator.

3.7 Uncertainty from the Experimental Apparatus

Though the reactor is operational and is capable of gasification and producing a syngas for analysis, uncertainty exists in the equipment used in the experiment. It is important to know how precise the equipment is in understanding accuracy of the results. A number of items can produce uncertainty and include: the amount of biomass inserted into the reactor by the feeder, the temperature recorded by the thermocouples, the bed temperature, the amount of steam entering the reactor, the volumetric flow rate of the gas meters, the pressure regulator and the gas composition recorded by the gas chromatograph. These uncertainties need to be included in the calculations to yield better results and a clearer standing of the reactor.

The feeder introduces biomass based on a volumetric rate. From the calibration tests, the feeder has an uncertainty of ±0.1 lbs per hour. Type K thermocouples are accurate to 2°F. The bed temperature had an oscillatory trend that was minimized as tests progressed but was able to hold a constant temperature with ±10°F. For all tests performed, the steam flow meter was held to a constant 5 lbs per hour. The steam rate fluctuated by ±0.2 lbs per hour at 50 psig, which is equal to ±0.15 lbs per hour at 30 psig.

Two types of gas meters were used in the experiments, large flow and small flow rates. The large flow meters were accurate to 1 cubic feet per hour, while the smaller ones were precise to 0.5 cubic feet per minute. The pressure regulator was set to 30±5 psig. Finally, the gas chromatograph measures the gas concentrations by volume percent and is accurate to 0.1%. These numbers were included during the data analysis and were used in the calculations and tables shown in the results section.

CHAPTER 4

THEORETICAL EXPECTATIONS

4.1 Approach to Theoretical Composition and Yields

Before experimental data is collected, knowing what theoretical approaches predict can be beneficial in understanding the actual results and in what way the experiment can improve. In the case of biomass gasification, the system can be checked by comparing the chemical compositions of the resulting syngas. A way to measure a theoretical gas composition is to determine the most stable arrangement for the molecules involved. Some arrangements are spontaneous and may give off energy, while other arrangements may increase the disorder of the system. Each arrangement of molecules has a different effect upon the energy within the system, sometimes increasing or decreasing it. Theoretically, each system seeks to achieve a minimum amount of free energy. If molecules are allowed to arrange themselves freely, the minimum required energy to maintain the system will prevail. This search for minimum point is often referred to as the minimization of Gibb's energy and is expressed in Equation (9). Once the minimum energy is found for a given set of molecules, the associated arrangement becomes the theoretical composition.

$$\Delta G = \Delta H - T\Delta S \tag{9}$$

There are several software packages that are capable of determining the minimization of Gibb's energy, but Aspen was selected for this experiment because of its availability and ease of use. Aspen already has a built in function that minimizes the energy for the specified molecules. The composition of syngas that comes from steam gasification can be calculated for a range of temperatures and pressure if the elemental composition of the fuel and possible syngas components are known. The U.S. Department of Energy has an available database that lists hundreds of types of biomass and their respective compositions. A table of the most common types of agricultural products used for gasification and the associated chemical composition can be seen in Table 2. It should be noted that this table only gives an average composition for each type of plant, which may vary depending on the climate, soil and seasonal changes. The different parts of a plant (bark, trunk, stems or leaves) have a different composition, as well.

Pine wood is a common biomass and one kilogram was specified in Aspen as the starting amount. The user cannot select pine from the list of available components, so the composition was entered as a gaseous mixture. The composition of pine from Table 3 was converted to moles and then arranged into molecules based on the available moles. The oxygen molecule was entered as O_2, sulfur was entered as H_2S, and carbon was entered as C_2H_2. The amount of hydrogen used in hydrogen sulfide and acetylene was subtracted from the total amount of available hydrogen. The remaining hydrogen molecules were inserted as H_2. Ash and nitrogen were neglected in the gaseous mixture since they are inert.

Aspen has a function that allows a user to specify all of the conditions except for a

Table 3. Chemical composition of biomass in weight percent commonly used in gasification.

This data was obtained from the U.S. Department of Energy

	C	H	N	O	S	Ash
Sugarcane	48.4	6.01	0.17	41.61	0.02	3.66
Corn Stover	47.04	5.47	0.68	41.1	0.06	10.24
Switch grass	47.27	5.31	0.51	41.59	0.1	5.76
Wheat Straw	43.88	5.26	0.63	38.75	0.16	10.22
Hybrid Poplar	49.75	5.52	0.52	42.42	0.03	2.03
Black Locust	50.36	5.71	0.54	40.62	0.03	2.08
Eucalyptus	49.89	5.71	0.05	42.29	0.01	1.22
Sycamore	49.73	6.15	0.25	43.79	0.03	1.24
Black Locust	46.03	5.86	0.88	41.37	0.12	9.68
Cottonwood	49.65	5.85	0.08	41.88	0.05	1
Pine	50.26	5.98	0.03	42.14	0.02	0.3
Average	48.69	5.76	0.37	41.66	0.06	3.47

single parameter which can be set as a range of values; this function is called selectivity and was used in this equilibrium analysis. Aspen will then calculate a series of experiments with the base data and a single value from the specified range until the entire range has been covered. For this equilibrium modeling, the physical property was defined as nonrandom two-liquid (NRTL) while the pressure was specified as 1 atmosphere. The temperature was stipulated as a range from 930-1830°F. Possible species were listed as H_2O, CO_2, CO, H_2, O_2, CH_4, C_2H_2, C_2H_4, C_2H_6, C_3H_6, C_3H_8, C_4H_{10}, SO_2, H_2S, CH_3SH, $(CH_3)_2S$, $(CH_3)_2S_2$, COS and CS_2. The results are presented in two subsections detailing the predicted compositions for the major species and hydrocarbons, and then finally an in-depth analysis of the compositions and trends of all major sulfur species.

4.1.1 Major Species and Hydrocarbons

The syngas is mainly comprised of hydrogen, carbon monoxide, carbon dioxide, water and methane, which are produced by reactions (1)-(4). However, two other gas-phase reactions are important for understanding the results and can be seen in reactions (10)-(11). It is important to note that these are not the primary heterogeneous reactions considered during gasification but are additional side reactions that play an important role on species compositions. Reaction (11) is commonly known as the water-gas shift and is reversible.

$$CO + 3H_2 = CH_4 + H_2O \quad (10)$$

$$CO + H_2O \Leftrightarrow CO_2 + H_2 \quad (11)$$

Figure 12 shows that at high temperatures carbon monoxide and hydrogen account for roughly 70% of the composition, but the concentrations decline sharply at temperatures below 1250°F to approximately 30%. At this temperature, reactions (10) and (11) have a more significant impact as they shift to the right, which almost eliminates carbon monoxide as a product. According to the consumption of carbon monoxide and the appearance of the other species, reactions (10) and (11) occur at a rate of 3 to 2. A rapid decrease in methane is present at temperatures above 1100°F as reaction 10 shifts to the left. All compounds could not be presented in this graph in order to obtain a clear understanding of the trends. Instead, the graphs have been organized according to major compounds, hydrocarbons, and sulfur species.

According to the minimization of Gibb's free energy, hydrocarbons are almost non-existent (except methane) and comprise less than 2% of the total composition at temperatures above 1250°F. However, analysis of these components is still beneficial and can be seen in Figure 13. The plot shows that at high temperatures, hydrocarbons with double and triple bonds are favored over those with single bonds by a smaller slope. However, all hydrocarbons decrease in concentration as temperatures increase, but molecules with single bonds disappear faster. These trends contribute to an increasing amount of energy within the system, leading to molecules that have higher energy bonds (C=C). At lower temperatures, the trend is the opposite. Hydrocarbons with at least one double bond show an initial increase in concentration at low temperatures. Of note, acetylene initially increases with temperature and then begins to decline at 1300°F at a

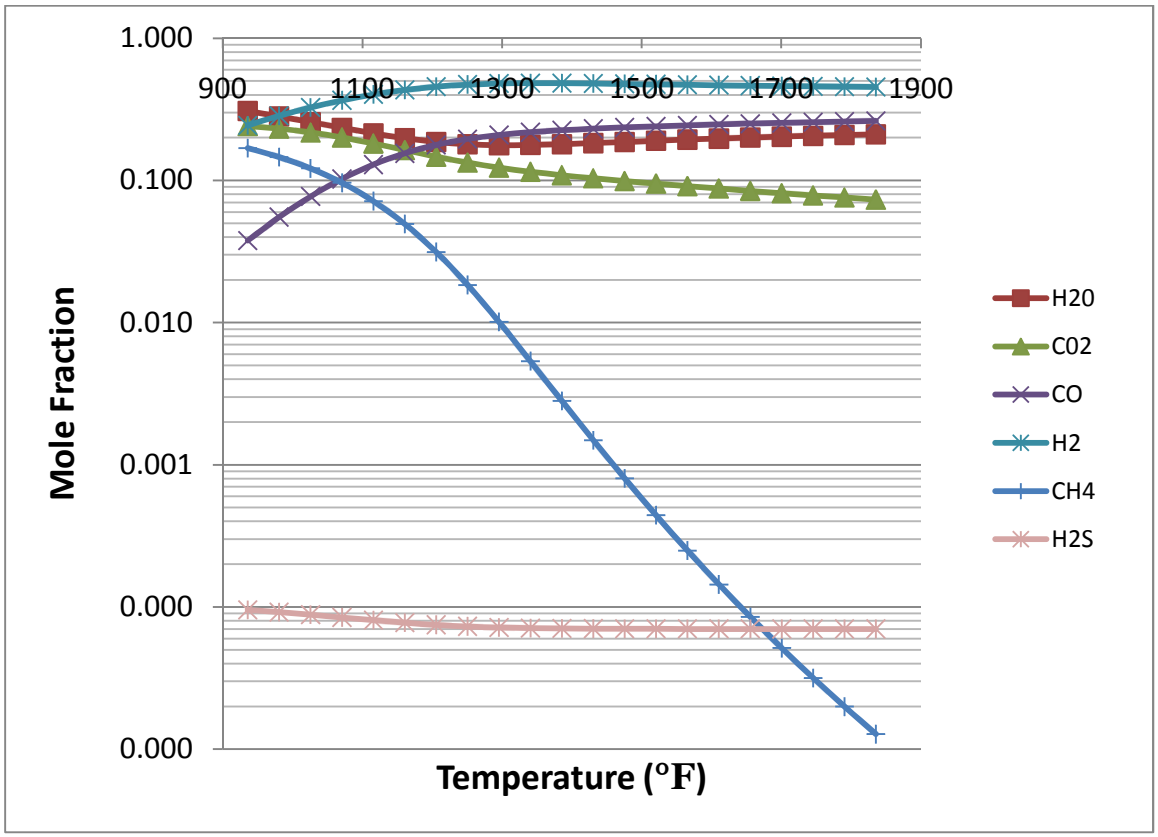

Figure 12. Theoretical yield of major components produced during gasification.

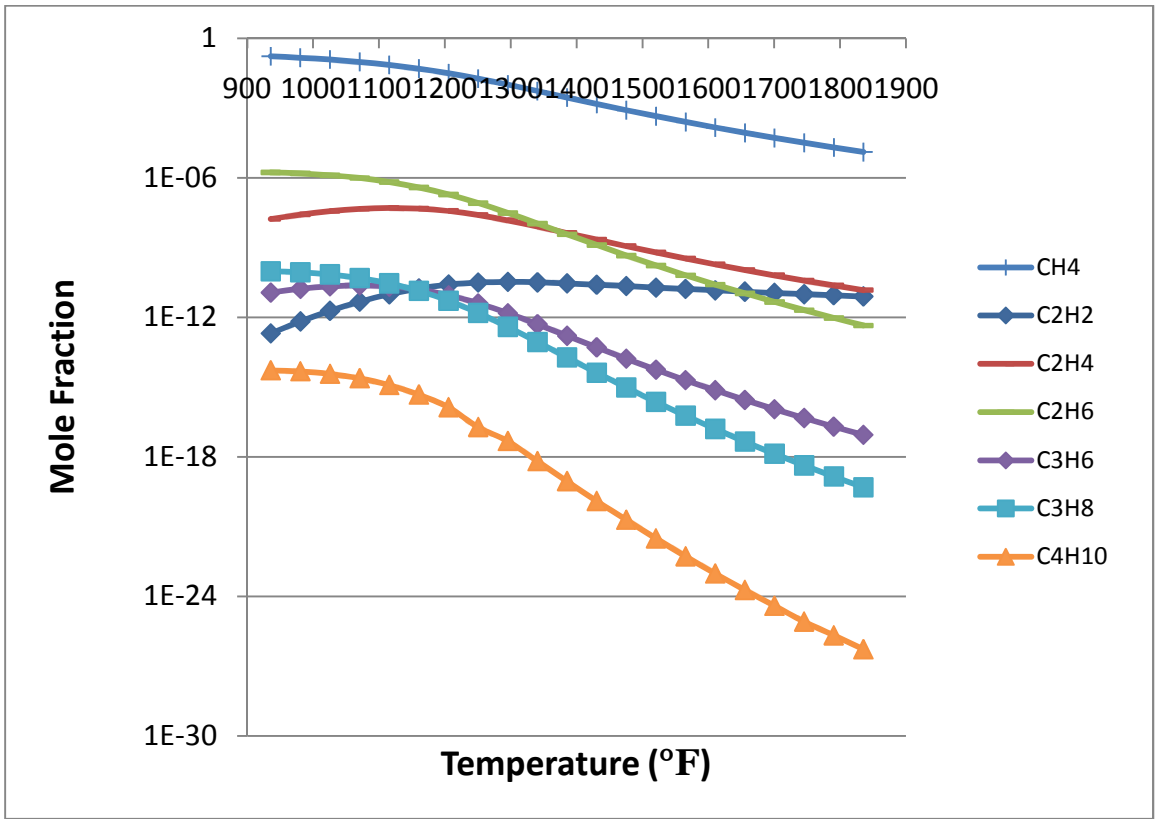

Figure 13. Theoretical yield of hydrocarbons produced during gasification.

slow rate. From the equilibrium plots, hydrocarbons that contain three carbons never appear as a major hydrocarbon. This can be explained by a very low C-C bond strength that is not favorable.

4.1.2 Sulfur Species and Trends

Figure 14 shows the theoretical yields of all species that contain sulfur. This plot shows that the majority of sulfur is contained within hydrogen sulfide and carbonyl sulfide. The concentration of hydrogen sulfide remains relatively constant and does not seem to show any correlation with temperature. However, hydrogen sulfide does decrease in concentration by a small amount at elevated temperatures; this amount of sulfur appears in a higher concentration carbonyl sulfide. At high temperatures, all compounds that contain hydrogen and sulfur decrease, while molecules that contain sulfur, carbon and oxygen show an increasing trend. This is likely caused by a more stable C=S and S=O bonds at high temperatures than the single H-S bond.

If hydrogen sulfide and carbonyl sulfide are neglected, a closer look at the remaining sulfur-containing species can be observed. At low temperatures, the concentration of methyl mercaptan is the overwhelming majority due to the high concentration of methane at these temperatures as seen in Figure 12. However, as the temperature increases and methane is swept away in favor of hydrogen and carbon monoxide, methyl mercaptan quickly disappears. Though steam gasification does not favor oxidation, sulfur atoms at high temperatures appear to pull oxygen atoms away from carbon monoxide and carbon dioxide.

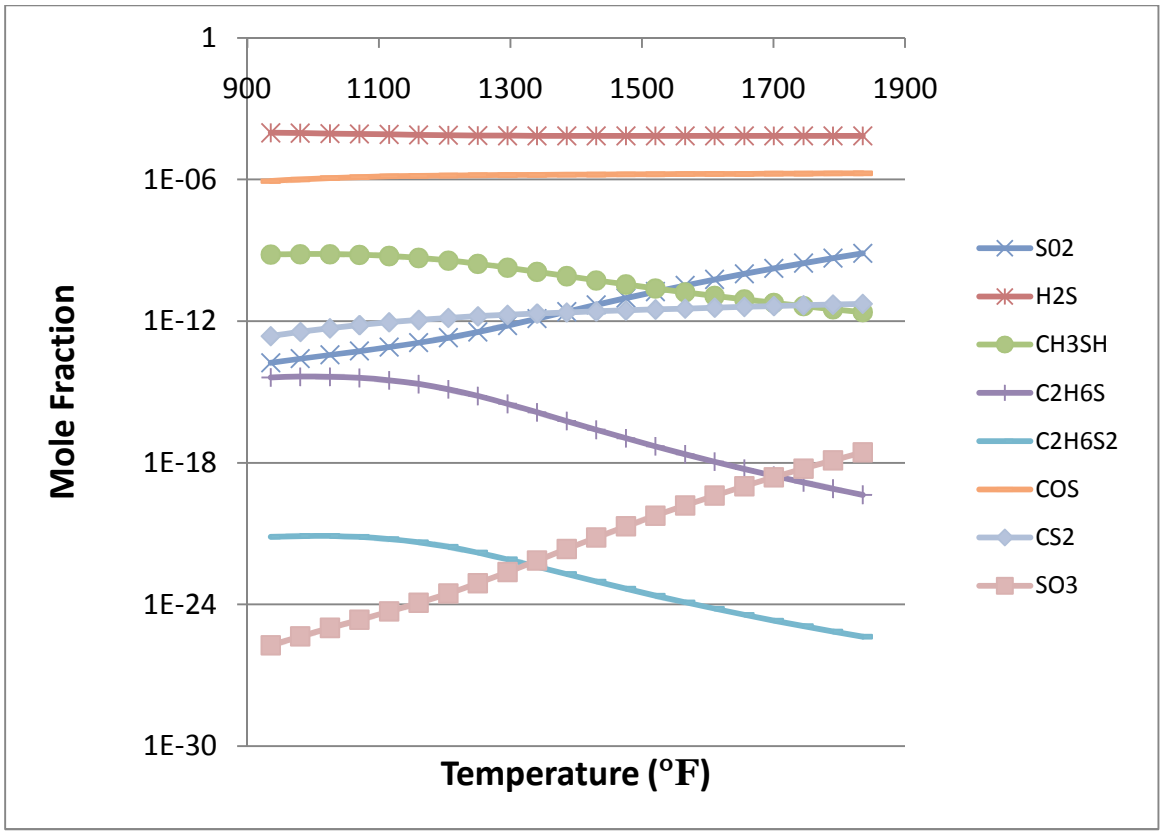

Figure 14. Theoretical yield of all species containing sulfur.

CHAPTER 5

RESULTS AND DISCUSSION

5.1 Total Syngas Quality and Composition

One of the major objectives of this research project was to establish a better sampling method for syngas analysis with an emphasis on species containing sulfur. Therefore, the sampling system underwent several revisions to optimize the quality and quantity of the resultant syngas stream. After each major modification to the reactor or sampling system, biomass was gasified to determine the progress of the sampling system, and if the water vapors, particulate matter and tars had been sufficiently removed. For progress comparison, an initial analysis on the syngas was performed after crudely condensing all tars and water in an impinger. The resultant gas composition can be seen in Figure 15. This is compared to the total gas composition obtained after the final sampling system was put in place and can be seen in Figure 16. The total amount of all minor gas components is listed as other.

Comparison of the two species profiles shows that a better composition was gained both qualitatively and quantitatively within the minor species. It is important to note that the conditions for both tests are very similar and that only changes to the sampling system and how biomass was introduced into the system were made while the reactor itself was unchanged. Qualitatively, the new sampling system was able to preserve methyl mercaptan, sulfur dioxide and several hydrocarbons from being

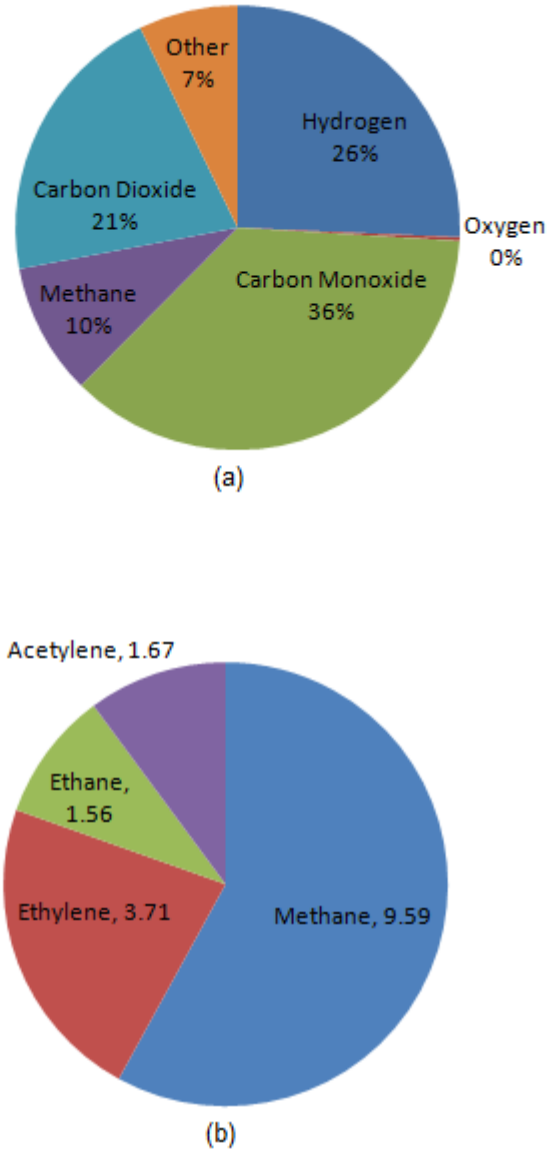

Figure 15. Total gas composition after using a crude water impinger sampling system. (a) major gas constituents and (b) the 'other' minor hydrocarbons. Produced from 1.5 lbs/hr switch grass at 1300°F with a fluidizing velocity of 0.3 ft/s.

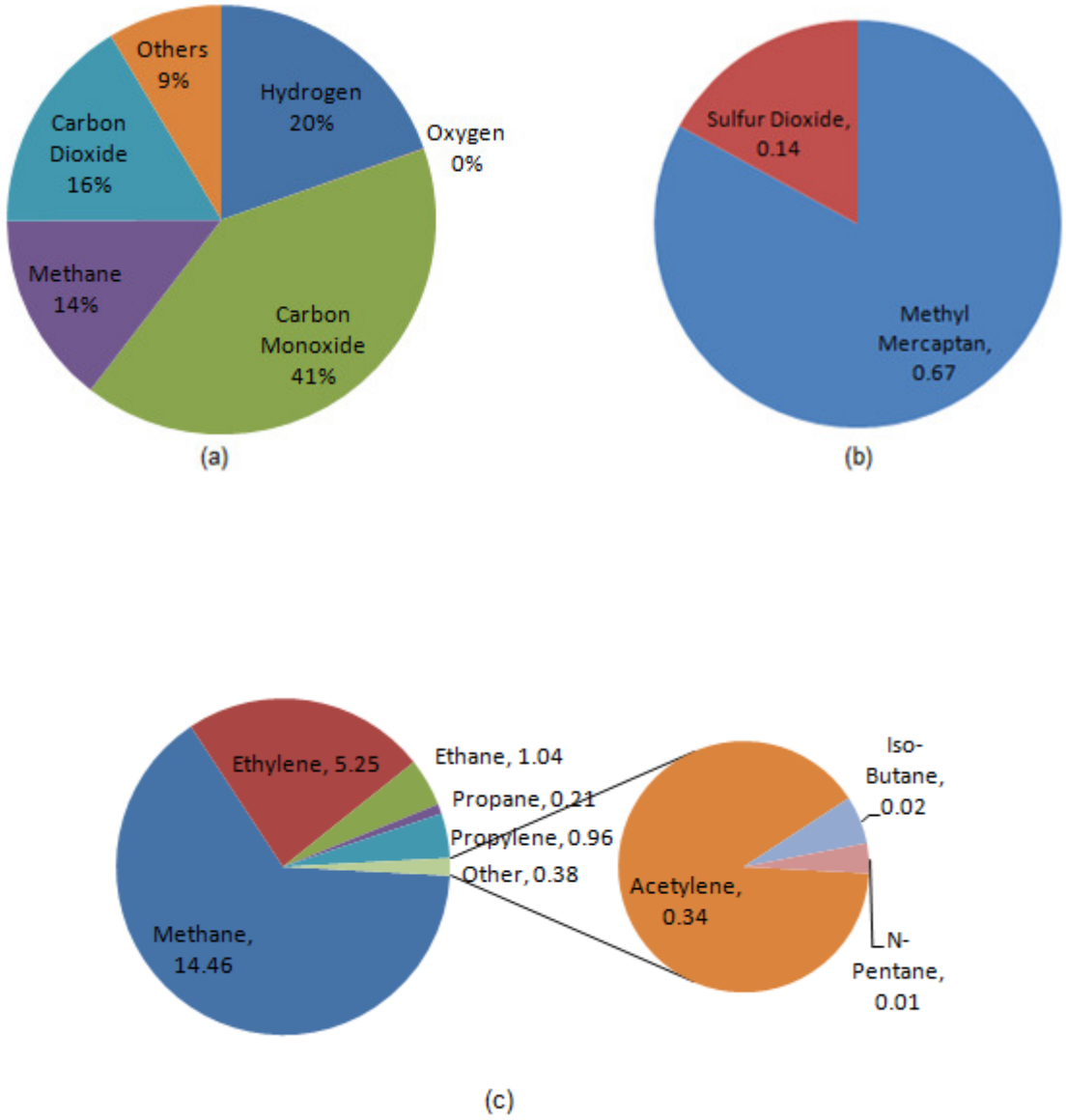

Figure 16. Total gas composition after the final sampling system was in place. (a) major gas constituents (b) sulfur species and (c) minor hydrocarbons. Produced from 1.5 lbs/hr switch grass at 1225°F with a fluidizing velocity of 0.3 ft/s.

condensed. Additionally, the sample system conserved four unknown compounds that were not identifiable by the gas chromatograph. The residence times of the unknown species appeared in the fourth column and show similar residence times as some heavier hydrocarbons such as pentane and hexane. These species could possibly be identified as a long hydrocarbon that has a double bond such as pentene or butylene. The most important aspect was the identification of species that contain sulfur, which shows that the dryer was capable of removing water during the gas phase. However, the gas chromatograph was not able to detect hydrogen sulfide and carbonyl sulfide, the two most abundant sulfur species predicted by theory.

Quantitatively, the sampling system appears to show an increased volumetric flow of hydrocarbons to the gas chromatograph, by preserving a portion that was previously condensed. This can be seen by contrasting the amount of methane, ethylene and ethane produced. However, the temperature of the reactor after the sampling system was set in place is roughly 75°F cooler. Equilibrium analysis shows that this temperature range is where the transition begins to occur for hydrocarbons with single or double bonds. Therefore, results based only off of these two graphs are inconclusive and do not necessarily represent an increase in recovered gas. Only one successful experiment was performed before the sampling system was corrected so only a small amount of data was available for comparison to the results obtained after the sampling system was modified. Another test at the same temperature and feedstock as the first sample seen in Figure 15 would need to be taken and has not been tested.

5.2 Identification of Syngas Compounds

One of the key objectives of this experiment was to successfully identify and measure the compounds in the syngas stream. An emphasis on identifying compounds that contain sulfur is a key experimental objective due to the high solubility of sulfur in water. Species identification was accomplished by comparing what the gas chromatograph identified as a certain compound to the residence times of the calibration gases. Additionally, the concentration and amounts of all the constituent gases are compared to the theoretical compositions.

Table 4 compares the residence times of calibrated gases against the residence times obtained by the gas chromatograph during operation. As previously mentioned, the gas chromatograph has four independent columns to identify compounds. In some instances, two columns are used to identify the same compound for an increased amount of accuracy although only one concentration is recorded for data analysis. It is also important to note that the gas chromatograph was setup with an error range of 0.2 minutes, meaning that a compound can fall within the time range and still be identified as a certain compound. The species in the table were arranged according to the residence times as well as the column from which the concentration was selected. It should be noted that some compounds in the second column have similar residence times as others. However, the sequence of the recorded compounds is important as they emerge from the chromatograph and prevented confusion.

A majority of the gas compounds have comparable residence times as the calibrated residence times. This closeness shows that the gas chromatograph was setup correctly and was capable of identifying the compounds. However, an even closer look

Table 4. Comparison of the calibrated and actual residence times of the gas chromatograph. The actual results were obtained at 1100°F at 1.25 lbs per hour of wood chips.

Name	Calibrated RT (min)	Actual RT (min)
Column 1		
Hydrogen	0.80	0.80±.01
Oxygen	0.97	0.98±.01
Nitrogen	1.09	1.13±.01
Carbon Monoxide	1.57	1.68±.01
Column 2		
Methane	0.28	0.29±.01
Carbon Dioxide	0.35	0.33±.01
Ethylene	0.4	0.36±.01
Ethane	0.44	0.38±.01
Acetylene	0.54	0.43±.01
Methyl Mercaptan	0.76	0.79±.01
Sulfur Dioxide	1.78	1.96±.01
Column 3		
Propane	0.29	0.25±.01
Propylene	0.33	0.29±.01
Iso-Butane	0.39	0.34±.01
Column 4		
N-Pentane	0.83	0.86±.01

needs to be taken at compounds that have a larger discrepancy than 0.1 minutes. Gases with this time discrepancy include carbon monoxide, sulfur dioxide and acetylene. Of these compounds, carbon monoxide is the most critical component since it is present in the largest concentration and was a key indicator that gasification was occurring. Looking at the recorded data during other experiments for carbon monoxide yields a range of residence times that fall within the error range. From an operational standpoint, residence times on the first column are known to shift towards longer times until the system is correctly cleaned. However, the main indicator is the concentration of this compound, which in all experiments was one of the largest, typically in the 30-40% range. If this concentration is compared to equilibrium numbers, the amount is comparable to the expected value and is considered to be carbon monoxide.

Acetylene was also detected in the third column with calibrated and actual residence times of 0.35 and 0.3 minutes, respectively. The concentration detected in both columns was identical. However, when compared to theoretical equilibrium expectations, the concentration was much higher but comparable to concentrations of other identified hydrocarbons. Additionally, the trends associated with acetylene follow the theoretical trends and are covered in subsequent sections. Nonetheless, it is reasonable to assume that this compound is acetylene.

The final compound identified by the chromatograph was sulfur dioxide and has the largest error when compared to the calibrated residence time. Additional experiments show the same recorded residence time with comparable concentrations. If this compound is compared with equilibrium concentrations, the numbers are not close. In addition, gasification produces a reducing environment which favors the formation of

hydrogen sulfide, carbonyl sulfide, etc. Sulfur dioxide is consistently produced in oxidation environments such as combustion but is not expected in gasification. Evidence suggested that this compound was not sulfur dioxide. However, there is a direct connection between the concentrations of this unknown compound and methyl mercaptan as they rise and fall together. This is covered in subsequent sections. Additional research shows that this residence time is comparable to ethyl mercaptan or dimethyl sulfide when contrasted against other sulfur species (Morehead et al., 2011). From this information, it can be concluded that this species is not sulfur dioxide but may be another sulfur species for which the gas chromatograph is not calibrated and will simply be called an unknown sulfur species throughout the remainder of this report.

5.3 Influence of Operating Conditions

To understand the reactor and sampling system better, a series of experiments was completed to test the newly built apparatus. To maximize the efficiency of the tests and minimize the amount of tests, only a few operating conditions or biomass selections were included in the analysis. Operating conditions which can be varied include fluidizing velocity, reactor temperature, steam flow rate, biomass feed rate and co-feed gases (nitrogen and carbon dioxide). Of those listed conditions, temperature and biomass feed rate were selected as the experimental variables because of their ability to generate significantly different results while still getting direct measurements from the gas chromatograph. Additionally, these variables are also the most accurate to control.

Three different biomasses were available for selection, including: sorghum, switch grass and pine wood. Pine wood and switch grass were selected as the feedstock

because of their different compositions as shown in Table 3. Switch grass and sorghum have similar compositions as they both contain a large amount of foliage; however, the composition of switch grass is more well-known and readily available in databases.

The ranges of temperature and biomass feed rate were selected from information gathered during the equilibrium analysis. Temperatures of 1100, 1225 and 1325°F were chosen because they lie within the transition range of the major gas constituents and should provide a range of data points. The feed rates of the biomass feedstock were selected on biomass-to-steam ratio. A steam flow rate of 3.5 lbs per hour entering the rotameter at 30 psig was selected based on observations of the bed dynamics. A range of biomass feed rates was selected to complement the fluidizing velocity but was limited by the volumetric output of the feeder, depending on the density of the biomass. Chosen feed rates were 1.0, 1.25, 1.5, 1.75 and 2.0 lbs per hour.

The volume of biomass feed proved to be the easiest of the variables to control, since the reactor took close to 45 minutes to equilibrate once the temperature set point was changed. Therefore, the reactor was run at each temperature while the feed rate of the biomass or type of biomass was changed. After each change in feed rate, the reactor and volumetric output were allowed to equilibrate; sampling for each condition would then commence for approximately 30 minutes and an average for the condition would be applied to the sampling data. With the experimental procedure defined, several experiments were performed to test the reactor and sampling system.

5.3.1 Variable Reactor Temperature

To see how the reactor operates during each of the variable conditions, parallels will be drawn and contrasted to the trends that occur according to theory. Many of the trends presented in the theoretical section can be seen by looking at Figure 17. The conditions set forth in that figure were to some extent considered the initial testing conditions (1225°F, 1.5 lbs per hour pine wood). From the plot, hydrogen and carbon monoxide combined represent roughly 63-67% of the resulting syngas stream, which falls within the range as seen by theory which changes from 55 to 70% over the same temperature range. Hydrogen and carbon dioxide increase while methane and carbon monoxide decrease. The trends associated with hydrogen and methane also mimic the trends found in theory. The presence of oxygen indicates a small leak, most likely through the pump, and is not included in the results; the associated nitrogen was also removed.

There is a large decrease in carbon monoxide and a small increase in carbon dioxide as temperature increases, which are contradictory to theory. At first glance, one could speculate that the compounds are behaving according to the water-gas shift reaction (11), though this does not explain the large discrepancy in carbon reduction. A small leak in the feed section was noticed during the test at 1100°F, which affected the gas composition at that temperature. This trickle may lead to incorrect trends in the gas composition. It should also be pointed out that the plot does not include water, a significant portion of the exit stream, because it could not be measured directly through the gas chromatograph.

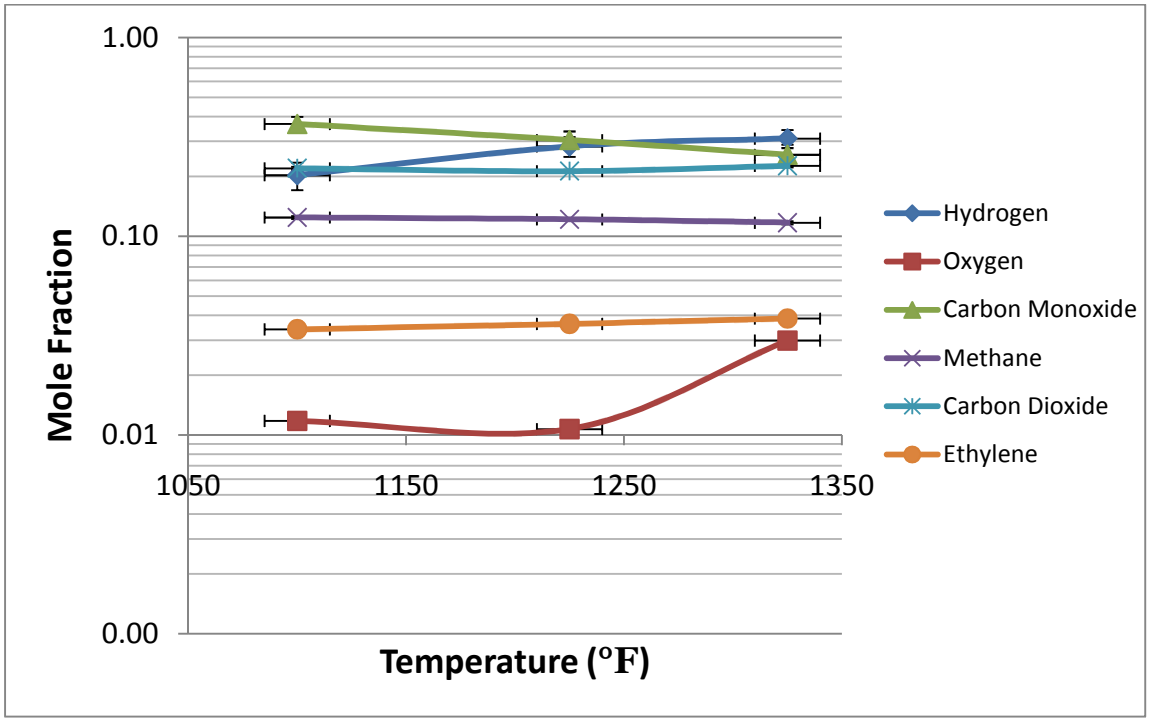

Figure 17. Yield of major syngas constituents with a feed rate of 1.5 lbs per hour of pine wood and 3.5 lbs per hour of steam.

Figure 18 shows the hydrocarbons in minor concentration as a function of temperature. The trend of hydrocarbons seems to resemble the theoretical trends to a better extent but does not have such a drastic decline. All compounds that contain only single-bonded carbons from the experimental data show a decline in concentration as the temperature increases. This is attributed to the formation of more stable double bonds between carbon atoms and between oxygen and carbon atoms. Theoretically all hydrocarbons should decline, single bonds faster than double etc., but the experiment indicated that there was an increase in concentration of acetylene and ethylene, compounds that contain only double and tripled-bonded carbon atoms. Long-chain hydrocarbons such as propane, propylene and pentane decline very rapidly, while ethane and methane do decline but at a smaller rate. If the temperature increased even further, the reduction in hydrocarbons would continue until depletion.

Sulfur containing species concentrations are presented in Figure 19. It should be noticed that only methyl mercaptan is present in the plot. According to equilibrium calculations, the most abundant sulfur species are hydrogen sulfide and carbonyl sulfide. The gas chromatograph used in this experiment was not calibrated for carbonyl sulfide but should have a residence time similar to residence times of the unknown species detected in the fourth column. Since hydrogen sulfide was not detected, though calibrated for, there is still an issue with condensation. Ways to correct this defect are outlined in subsequent sections. The trends of methyl mercaptan compare reasonably with theoretical expectations, with the concentration of methyl mercaptan decreasing rapidly as temperatures increase. This is attributed to the weak C-H and S-H bonds

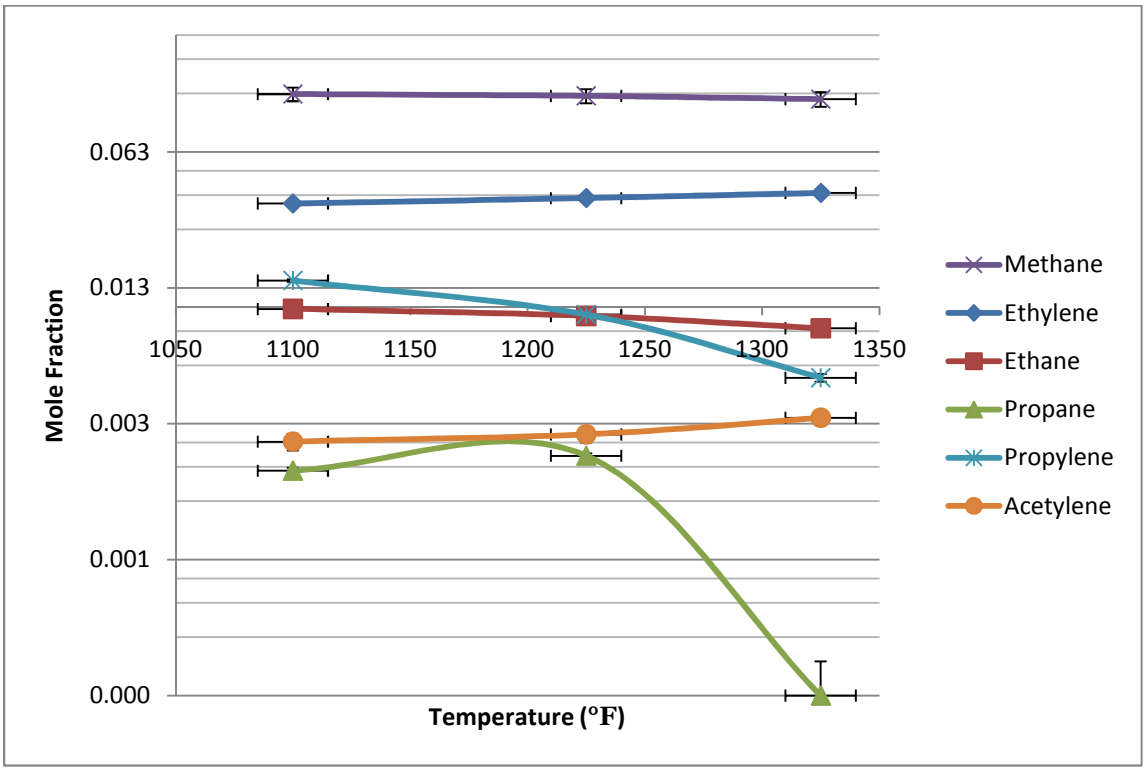

Figure 18. Yield of minor hydrocarbons with a feed rate of 1.75 lbs per hour of pine wood and 3.5 lbs per hour of steam.

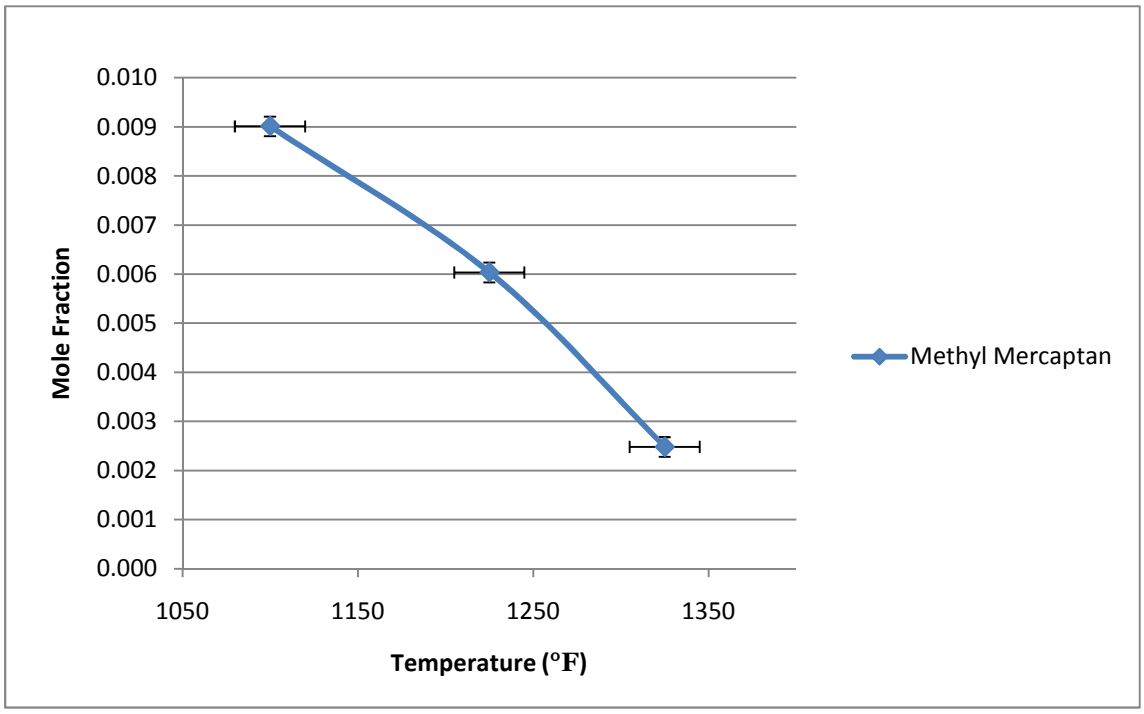

Figure 19. Yield of sulfur containing species with a feed rate of 1.75 lbs per hour of pine wood and 3.5 lbs per hour of steam.

which are easily replaced by stronger C=H, C=O and C=S bonds. However, the concentration of methyl mercaptan is much higher than expected.

5.3.2 Variable Biomass Feed Rate

The feed ratio of steam-to-biomass is important for determining the best operating conditions for a particular reactor. The aim of this section is to determine the best biomass feed rate for the 4-inch bench scale gasifier. Several tests were performed with each experiment yielding similar results, which can be seen in Figure 20. This plot shows a direct connection between the major gases produced through gasification by their relative increases and decreases. This correlation between carbon monoxide and hydrogen shows the influence of the water gas shift reaction (reaction 11). The concentration of carbon dioxide decreases with the decline in hydrogen, but to a lesser extent. The location of where the concentrations cross is not significant, since a clear connection between the extent of water gas shift and the amount of biomass injected into the reactor can be established from the data. However, the total combined amount of hydrogen and carbon monoxide increased as more biomass was added to the reactor, showing that more hydrogen and carbon monoxide were produced as the feed rate is enlarged.

As the amount of biomass increases, the formation of methane went up due to an increase in the availability of carbon atoms for chemical reactions. As the temperature was changed to 1100 or 1325°F, the total percent of hydrogen, carbon monoxide and carbon dioxide decreased and increased, respectively, revealing the same trends seen in Figure 9.

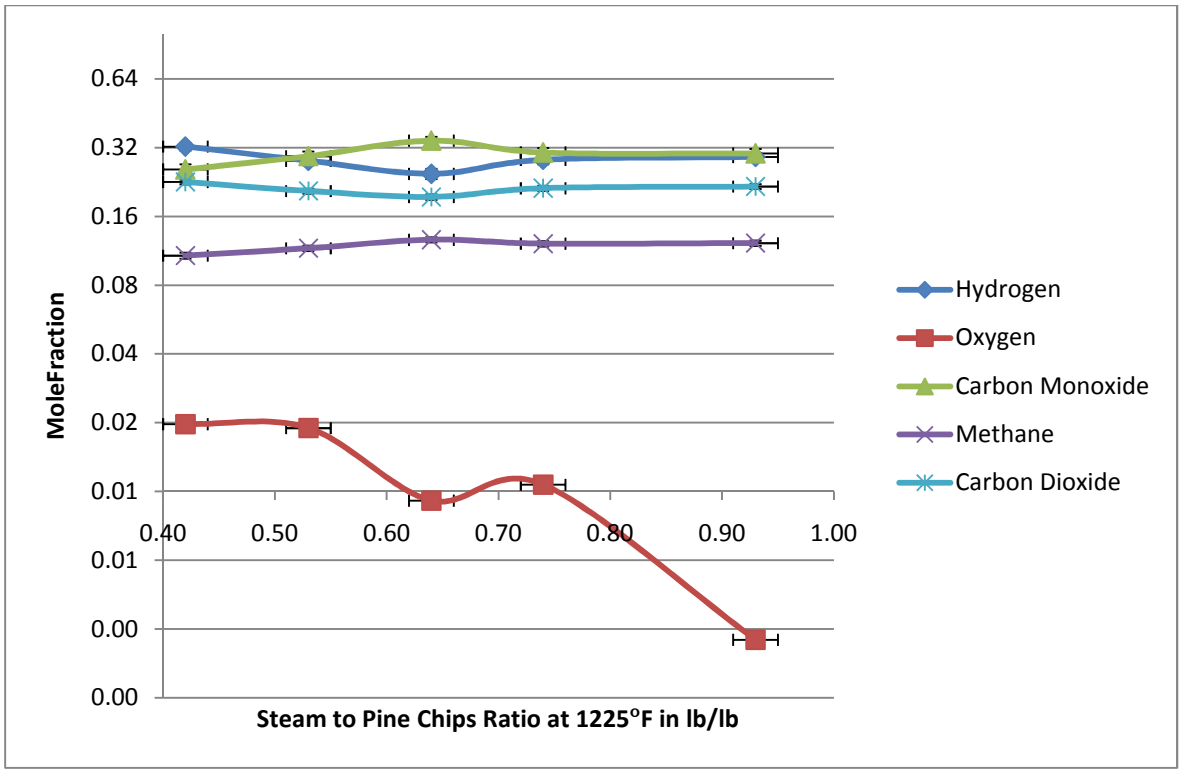

Figure 20. Yield of major gas constituents as a function of biomass feed rate in lbs per hour with constant flow rate of steam at 3.5 lbs per hour.

The concentration of hydrocarbons did not seem to be affected much by increasing the biomass feed rate. Most species have a concentration that is stable despite the increased amount of fuel as seen in Figure 21. However, the lone exception was the reduction in propane; there is not a clear understanding to this trend. Even at the other temperatures (1100 and 1325°F), the concentration of the hydrocarbons remains comparatively the same. It should be noted that though the concentration of the hydrocarbon species is not increasing, the volumetric amount increases as more biomass is fed.

The sulfur-containing species and the associated development with biomass feed rate can be seen in Figure 22. The most interesting trend in that plot has nothing to do with the concentration, but is the connection between methyl mercaptan and this unknown species. The trends of these two compounds mirror each other and suggest that their concentration is dependent upon the other. If their relative concentrations are summed together, they yield a relatively constant concentration. This summation does not differentiate more than 5%, revealing a strong connection between the species, which suggests that the unknown species may contain sulfur. However, the concentration of these species did not increase with an increasing amount of biomass, and no conclusion can be drawn according to this variable operating condition.

Though the concentration of all species is relatively constant, it is worth mentioning that the amount of all species increases with the volumetric flow rate, which can be seen in Figure 23. The plot shows both an increasing production rate in temperature as well as biomass injection. These correlations pass a logical analysis as higher temperature should produce a higher conversion rate, while an increase in fuel

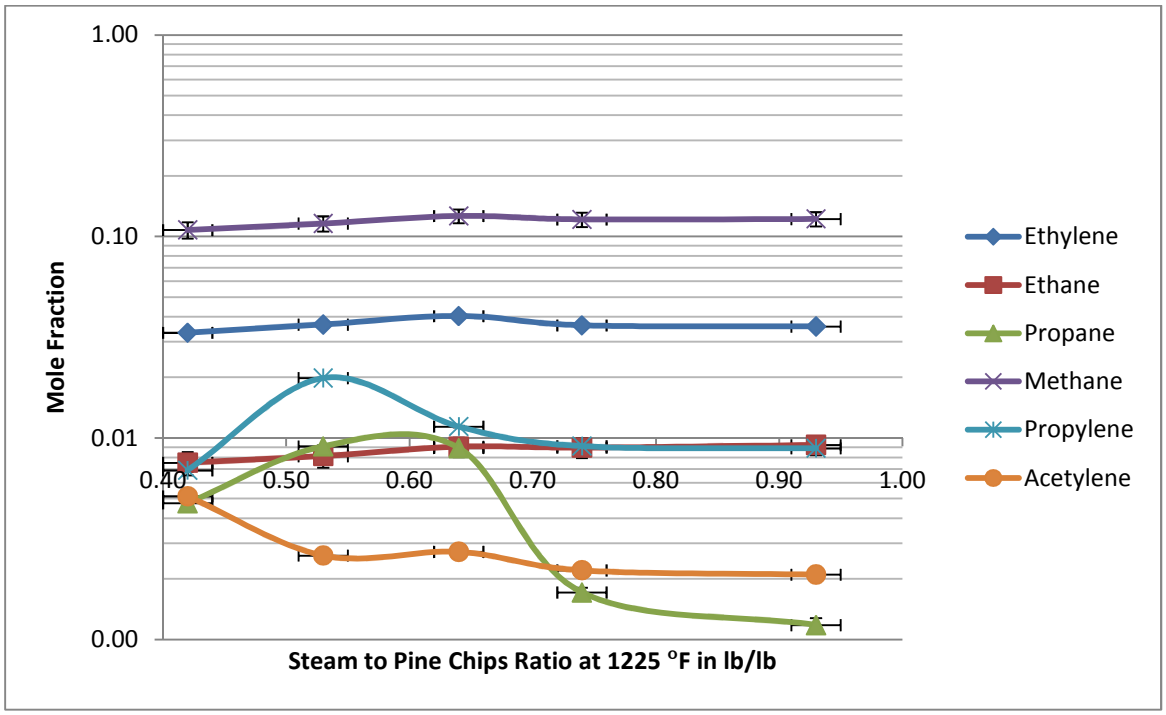

Figure 21. Yield of minor hydrocarbons as a function of biomass feed rate in lbs per hour with constant flow rate of steam at 3.5 lbs per hour.

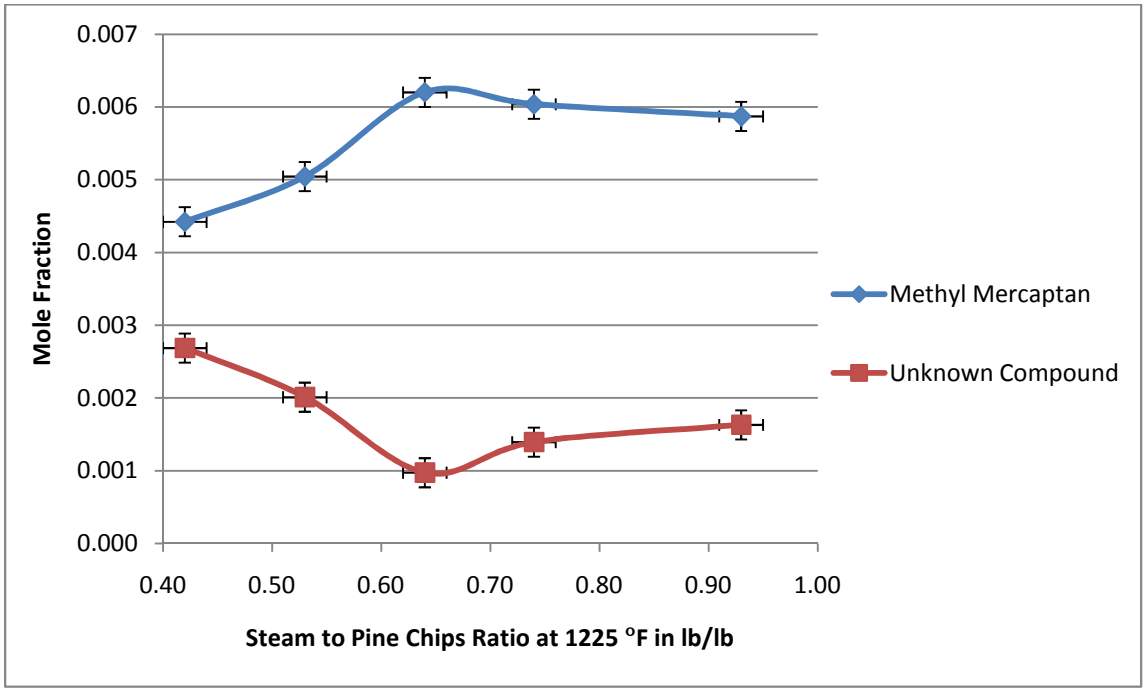

Figure 22. Concentration of sulfur species as a function of biomass feed rate in lbs per hour with constant flow rate of steam at 3.5 lbs per hour.

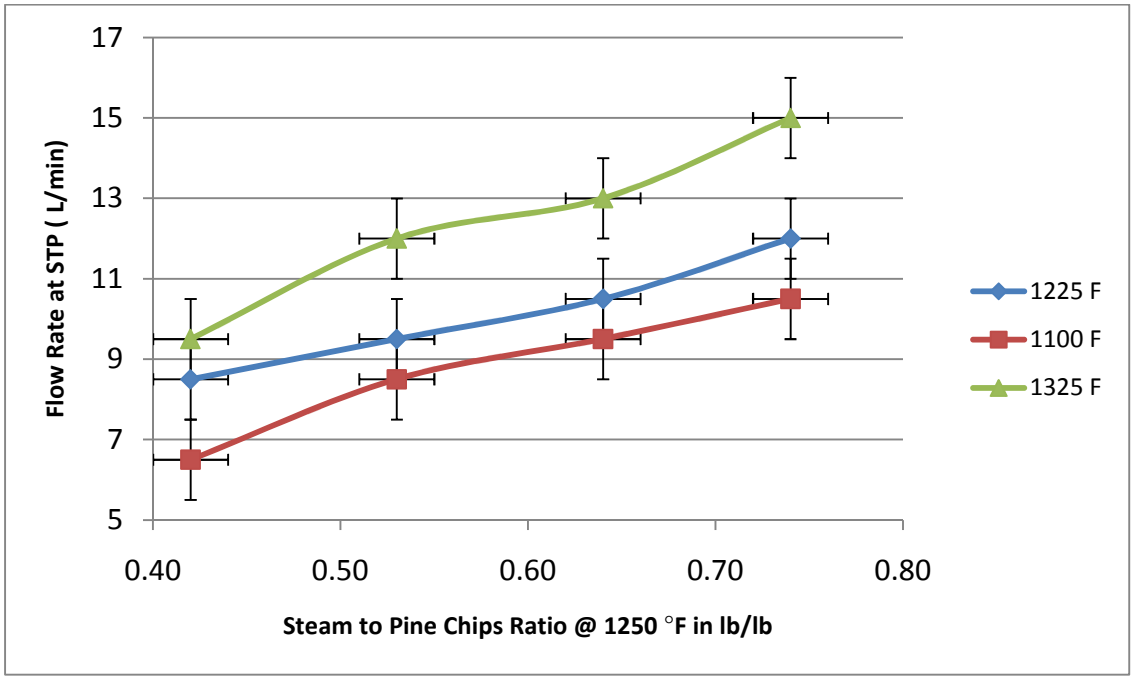

Figure 23. Volumetric flow rate of dry syngas for each temperature as a function of biomass feed rate in lbs per hour with constant flow rate of steam at 3.5 lbs per hour.

should produce a higher volumetric output. This graph does include the one liter per minute that was pulled from the stream for sampling.

5.3.3 Variable Biomass

The last variable is the results from different biomass materials. An analysis of the resulting gas composition for switch grass has already been shown in Figure 16; this information can be compared to the gasification results of pine chips under similar operating conditions, which are shown in Figure 24. At first glance, it is not any coincidence that the gas compositions of the two materials are very similar, especially considering the elemental composition shown in Table 3. Biomass has the innate characteristic that they are all carbonaceous fuels with similar biological processes that are used in creating them. The major elements found in both materials (carbon, hydrogen and oxygen) have similar percentages. The chief difference lies within the trace elements, such as nitrogen, sulfur, ash and other minerals. These trace elements are found in higher concentration in foliage because they are more critical for cell reproduction than for the cells that comprise the rigid plant structure. This is shown in greater detail in Table 5 (Richardson, 2002). Switch grass has a higher amount of these elements because of its leafy nature.

In both plots, the composition of the major gas components is similar. Hydrogen, carbon monoxide and carbon dioxide comprise roughly 80% of the entire gas stream. However, the pine chips were able to produce a higher volumetric rate of gas, 9 liters per minute as opposed to 6.5 liters per minute for switch grass. This difference was attributed to a higher conversion achieved from a higher particle density of pine chips. A

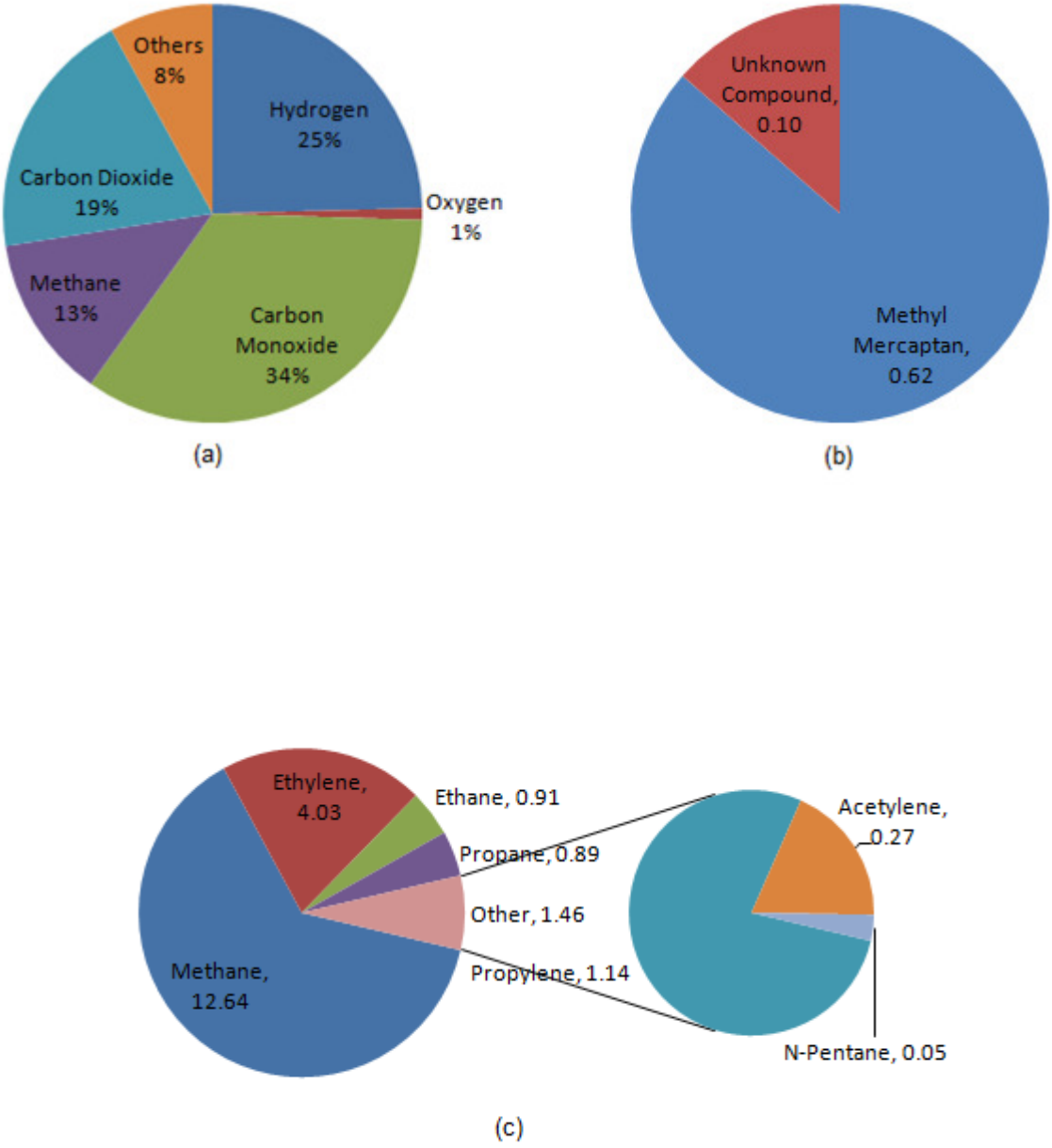

Figure 24. Total gas composition. Specifically, (a) major gas constituents (b) sulfur species and (c) minor hydrocarbons. Produced from 1.5 lbs/hr pine chips at 1225°F with a fluidizing velocity of 0.3 ft/s.

Table 5. The amounts of trace elements in various portions of biomass (adapted from Richardson et al., 2002).

Part of Tree	Elemental Amount			
	Mangenese	Iron	Zinc	Sulfur
	Concentration, mg per kg			
Softwoods				
Stem wood	147	41	13	116
Stem bark	507	60	75	343
Branches	261	101	44	203
Foliage	748	94	75	673
Entire tree	296	85	30	236
Hardwoods				
Stem wood	34	20	16	90
Stem bark	190	191	131	341
Branches	120	47	52	218
Foliage	867	135	269	965
Entire tree	83	27	39	212

portion of switch grass was elutriated by the syngas and water vapor and carried downstream. This carryover eventually caused the impinger to plug with char and ash preventing the collection of a sufficient amount of data for comparison.

In terms of the concentration of hydrocarbons and sulfur species, the pine chips produced a smaller amount of these products except for propane and propylene. This can be credited to the additional time for conversion that the pine chips had. Additionally, the figures show that the pine chips produced a smaller amount of sulfur species than switch grass, which was to be expected; however, the concentrations by comparison are much more similar than the elemental composition indicates. Data for a complete analysis and understanding of the results of the different biomass are inconclusive and deserve additional testing.

5.4 Carbon and Sulfur Balances

In order to understand the performance of the reactor better, carbon and sulfur balances were performed for each set of conditions. This type of calculation is also important for performing a material balance and for determination of fuel conversion. Performing these calculations requires consistent measurements of all materials that enter and leave the reactor. Locations where measurements were collected include: the gas chromatograph, bed particles, condensing water in the impinger and the two filters placed before the Perma Pure dryer and dry gas meter. Some of these points are impossible to measure during the actual experiment and the necessary information was collected after the experiments concluded and the system had cooled to ambient temperatures. Being

able to measure these outlets only once per experimental run results in uncertainty for each condition.

The gas chromatograph provided syngas composition several times during each condition. These numbers were averaged for a given set of conditions. Every five minutes throughout each operating condition, the flow rate to the gas chromatograph and through the dry gas meter was measured, recorded and then averaged. The amount of carbon and sulfur leaving through the syngas was calculated from the recorded composition by the chromatograph, molecular weights, the duration of each condition and the volumetric flow rate through the dry gas meter and sampling system. This calculation provides the weight of carbon that left the reactor. The amount of carbon and sulfur introduced into the reactor was determined by the feed rate, time and elemental composition from Table 3. These numbers were then compared in Table 6 showing the amount of carbon emitted for each condition as well as the converted percent.

This computation shows some significant trends. The most predictable trend is shown by comparing the temperature values; at each increasing temperature increment, the conversion of carbon increased showing that high operating temperatures led to a higher percentage of gasified biomass. The second trend is from the steam-to-feed ratio which illustrates a significant decrease in conversion as the amount of biomass is increased. This does not mean, however, that the best operating conditions are a high temperature and very little biomass; the main concern within industry is output since subsequent processes need a stable volumetric flow rate. This table is shown only for optimization purposes.

Table 6. Carbon contained in the syngas and the percent converted for each feed ratio and temperature of pine chips. Steam was held constant at 3.5 lbs per hour.

Temp	Steam to Feed Ratio	C (g/liter)	Flow (L/min)	Total C (g)	Feed (lbs/hr)	Feed C (g)	C converted
1100 F	0.42	0.16	15.5	60.4	1.00	94.9	63±3%
	0.53	0.16	17.5	98.4	1.25	166	59±3%
	0.64	0.18	18.5	82.6	1.50	142	58±2%
	0.74	0.17	19.0	99.6	1.75	199	49±2%
1225 F	0.42	0.17	18.0	89.3	1.00	114	78±3%
	0.53	0.20	18.5	111	1.25	142	78±3%
	0.64	0.23	19.5	88.0	1.50	112	77±2%
	0.74	0.20	21.0	104	1.75	166	63±2%
	0.93	0.20	22.0	110	2.00	189	58±2%
1325 F	0.42	0.17	19.0	80.8	1.00	94.9	85±3%
	0.53	0.18	21.5	94.5	1.25	118	79±2%
	0.64	0.19	23.0	109	1.50	142	77±2%
	0.74	0.19	25.0	163	1.75	232	70±1%

A similar table for the conversion of sulfur was calculated, but adds little help to the analysis and is not included in the report. The table confirms that sulfur species concentrations within the syngas were too high. Data analysis also showed a large amount of sulfur continued to be produced after the biomass feed was turned off. The unsubstantiated amount of sulfur is most likely contributed to an overestimate in composition from the gas chromatograph or the presence of sulfur in a piece of equipment. It is possible to point out that as the temperature and feed rate are increased, the measured sulfur concentration more closely matched expectations. However, the excessive nature of these values renders this point moot. It is speculated from Table 3 that the concentration of sulfur should be less than 0.01% of the gas composition if all of the inserted sulfur was converted to H_2S.

Additional tests were performed to identify the amount of carbon in the impinger, filters and bed material. The material that was recovered from each of these areas was hard to identify and the exact elemental composition was unknown. It appeared that this material was a mixture of char, ash and condensed tars. The substance should contain a considerable amount of carbon and was speculated to be such for simplicity during these calculations.

After the experimental runs, a small sample of bed material was recovered before and after air was added to the system. These samples were weighed and the resulting difference is assumed to be carbon, an additional 0.033 grams of carbon per mL. Knowing the volume of the bed material, it was estimated that an additional 30.5 grams of carbon were left in the bed after each run. Photographs of the bed particles before and after the analysis can be seen in Figure 25. Comparison of the particles show that there is

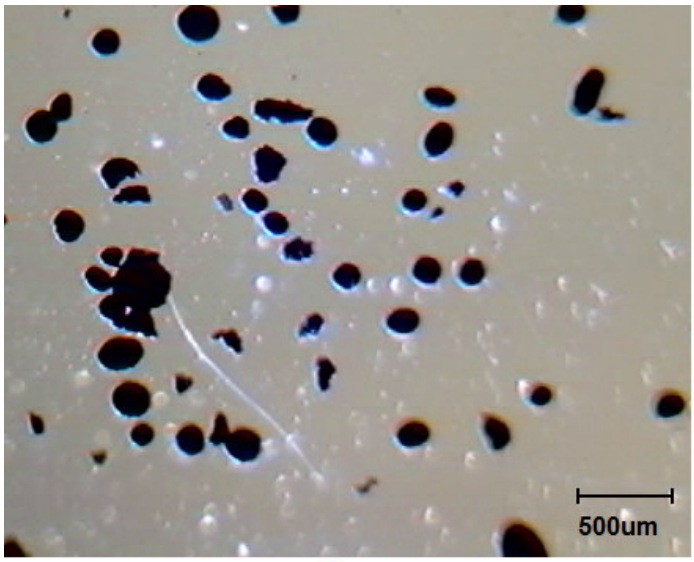

(a)

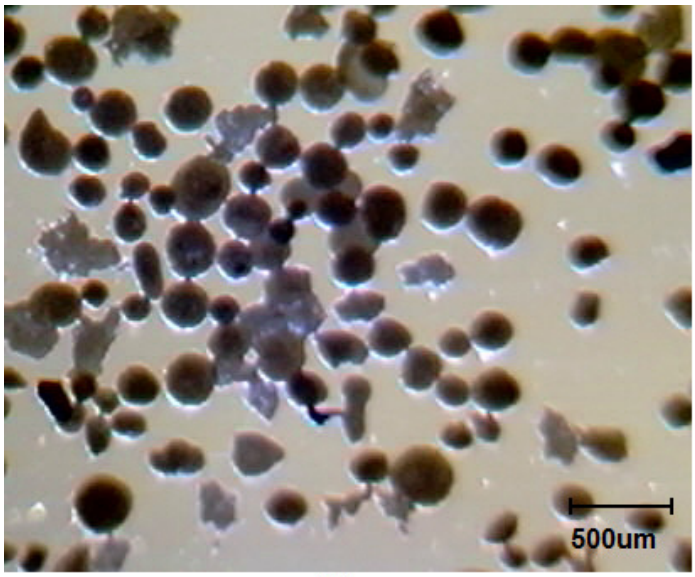

(b)

Figure 25. Bed particles collected from the fluidized bed

(a) before oxygen is inserted and (b) after it is inserted.

a higher concentration of carbon on the particles before oxygen was inserted into the reactor.

Also, the flow rate of cooling water to the impinger was held at 1 liter per minute. After each experiment a sample of water was collected, decanted, weighed and allowed to dry before weighing again. An additional amount of 0.41, 0.34 and 0.23 grams of carbon were recovered per liter for temperatures of 1100, 1225 and 1325°F, respectively. The duration of test, flow rate of water and concentration was used to determine the carbon in the impinger, 95.5, 89.7 and 53.6 grams for the aforementioned temperatures.

Finally, the change in weight of the filters before the dryer and dry gas meter were measured. Interestingly, the weight of these filters did not seem to change much between the experiments and added roughly 5 and 13 grams. If all of these carbon weights are added together, they still do not equate to 100% of the carbon inserted but elevate the amount of carbon in Table 6 by approximately 17-25%. This brings the total carbon for each temperature to approximately 88% of the inserted amount. Lower temperatures showed less carbon escaped from the reactor than higher temperatures and was attributed to an increase in tar. This number is based off of the total carbon for each temperature scenario because it is impossible to collect filter and bed samples during each feed condition.

The remaining carbon is speculated to be in the form of tars which were not measured during the project. The experimental apparatus did not have an adequate way to measure tars that were formed. Tars likely remained in the apparatus, condensed on the tubing walls, or were present in the impinger cooling water that was carried out. Certain sections of the tubing, filter and impinger were observed to contain tars but an

exact weight or amount cannot be accurately calculated. For these reasons, the concentration and amount of tars were not tracked or included in this project.

5.5 Comparison of Equilibrium Calculations and Results

It is important to evaluate the reactor performance by contrasting the equilibrium calculations in order to know how the apparatus differs. The reactor is not expected to yield the exact numbers as a minimization of Gibb's free energy because there are limiting factors such as residence time, kinetic rates and surface area. A plot of the major constituent gases for the experimental results and equilibrium calculations can be seen in Figure 26. The equilibrium calculations are represented by a dashed line and the chemical formula while the experimental results have a solid line and compound name.

The first observation is that the major compounds found in the experimental results lie within the same order of magnitude as the equilibrium calculations. Hydrogen is at half of the concentration as at equilibrium but the trends are almost an exact duplicate. Carbon monoxide shows the exact opposite trend and continues to decline with temperature; this is speculated to be influenced by the water gas shift reaction. The concentrations of methane and carbon dioxide are higher than the expected results but show a similar decline. However, the decline for these two species is at a much lower rate. Oxygen increases with temperature and compares nicely with the equilibrium calculations. The experimental results also show that the fraction of oxygen in the gas stream is approximately one percent while the equilibrium numbers show a much smaller amount.

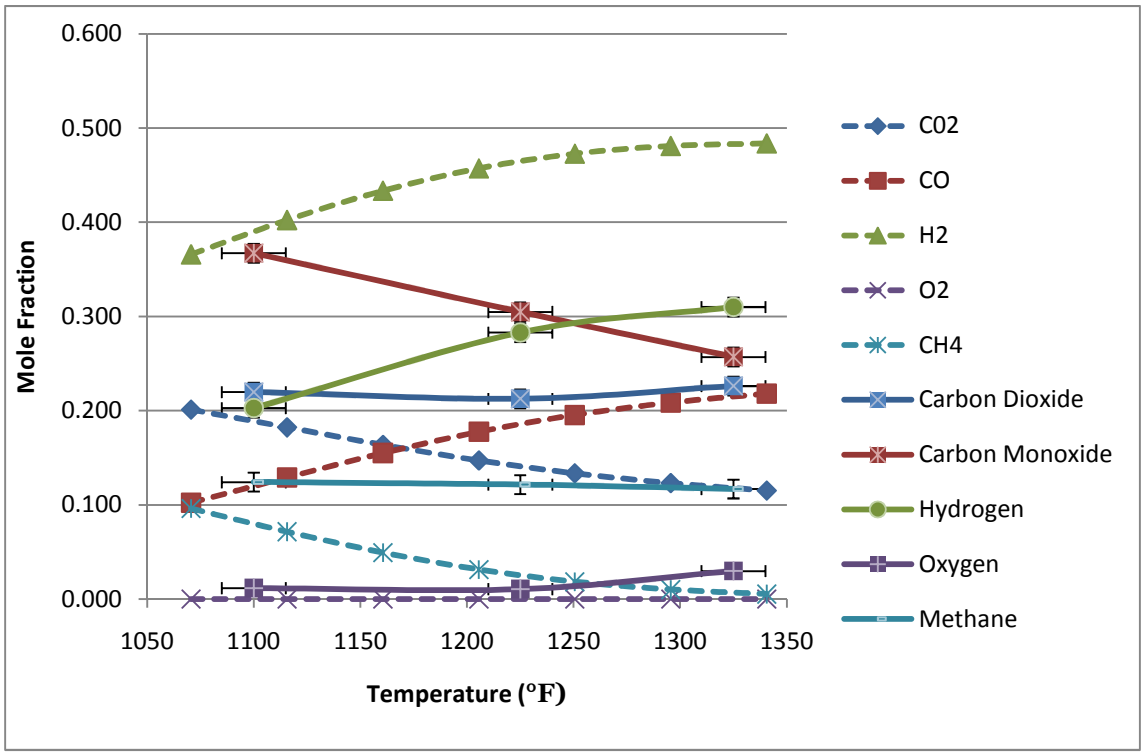

Figure 26. Comparison of the major gas constituents from equilibrium calculations (dashed line) and experimental results (solid line) as a function of temperature. Experimental results are from pine chips fed at 1.75 lbs per hour and a steam flow rate of 3.5 lbs per hour.

The hydrocarbons do not compare as favorably to the equilibrium calculations as the major gas components in terms of concentration. However, the associated trends of the hydrocarbons compare much better than the major gas compounds as seen in Figure 27. All hydrocarbons show a decrease in concentration as temperatures increase except for acetylene, which increases slightly. In both groups of compounds, hydrocarbons with single bonds decrease the most while carbons with double bonds decrease more slowly. Propane decreases by the largest amount in both cases. The only compound containing sulfur (methyl mercaptan) also decreases in both cases.

However, the major cause for concern is the discrepancy in several orders of magnitude between the equilibrium concentrations and the experimental results. A likely explanation is that biomass is dropped into the top of the reactor rather than being inserted directly into the bed. This results in less time for conversion and possibly devolatilization of the biomass. Additionally, once the syngas leaves the reactor, there is a sharp decline in temperature from 1250 to 600°F. These low temperatures favor the formation of hydrocarbons, especially methane as seen in Figure 12. The gases can also re-equilibrate when the temperature drops again through the sampling system that operates at 250°F. Additional tests are needed to deduce that these temperature drops are the source for the increased concentration of hydrocarbons in the sample stream.

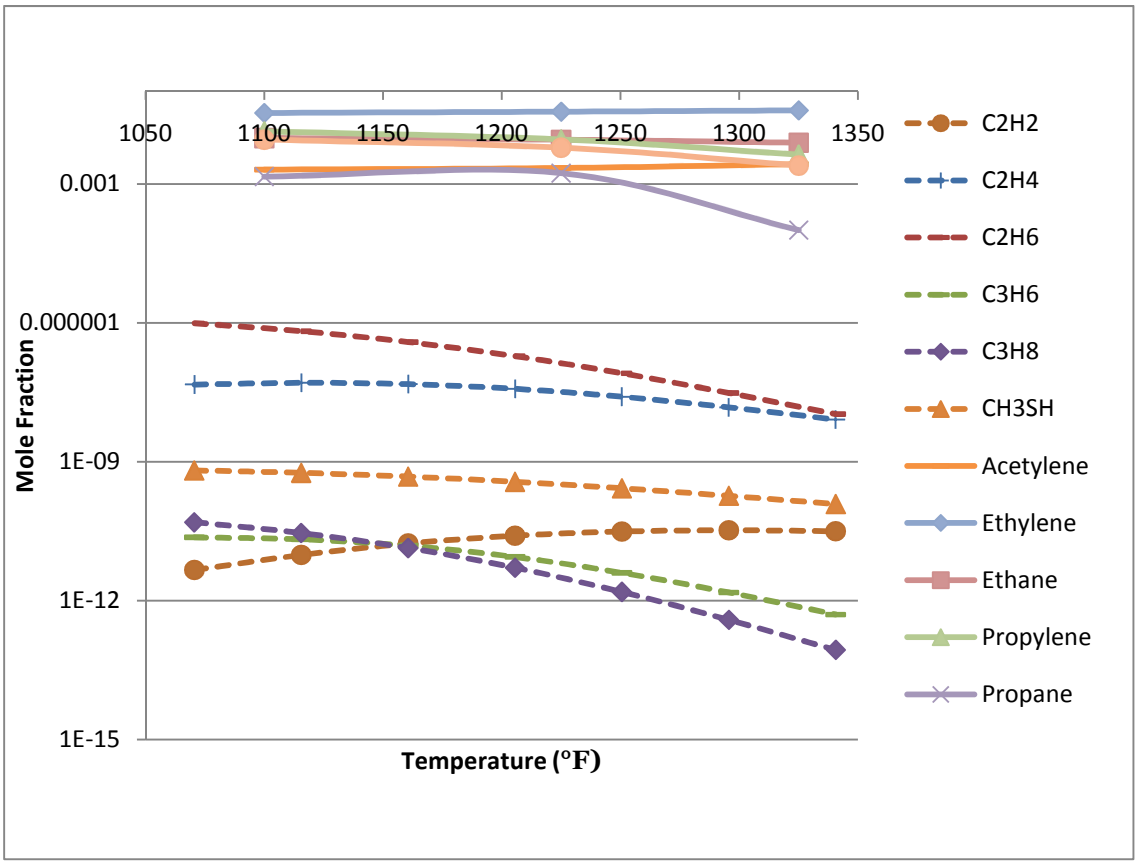

Figure 27. Comparison of the minor gas constituents from equilibrium calculations (dashed line) and experimental results (solid line) as a function of temperature. Experimental results are from pine chips fed at 1.75 lbs per hour and a steam flow rate of 3.5 lbs per hour.

CHAPTER 6

CONCLUSIONS AND RECOMMENDATIONS

6.1 Reactor Design and Condition Response

The reactor has similar concentrations of hydrogen and carbon monoxide and the trends associated with these major gas constituents are comparable to theoretical predictions. The measured concentrations did show an excessive concentration of hydrocarbons and sulfur containing compounds when compared to their modeled counterparts. This discrepancy is likely a consequence of the small residence time in the reactor since biomass is inserted into the top of the reactor. So, the gas presumably did not have enough time to reach equilibrium and the gas contained comparatively large concentrations of pyrolysis products. Gas compositions did illustrate the water gas shift reaction as the concentrations of carbon monoxide, hydrogen and carbon dioxide fluctuated in harmony.

Increasing temperature resulted in an increase in the volumetric flow rate of the syngas as well as a higher conversion percentage. Higher temperatures did result in more release of hydrogen and a smaller amount of hydrocarbons which mimics the trends found when compared to theory. However, the concentration of carbon monoxide did not increase with temperature while carbon dioxide and methane remain mostly constant with only a small decrease.

Increasing the amount of biomass did not seem to change the relative concentrations of the gases. The volumetric flow rate of the syngas did increase significantly as more biomass was introduced but also yielded a decline in carbon conversion. The conversion of biomass for all of the operating conditions varied between 49 and 85% depending on the temperature and feed rate and seems reasonable for a small gasifier in the range of temperatures studied. Conclusions about varying the biomass between switch grass and pine chips could not be drawn because of inconclusive evidence. This is due to a lack of successful experiments with switch grass and the comparable compositions between the two feed stocks.

Comparing the equilibrium calculations with the experimental results showed that the relative concentrations of the major gas constituents compared favorably. The amount of experimental compounds produced when compared to increasing temperature and equilibrium conditions showed conflicting trends. The concentration of these compounds may also suggest a larger influence by the water gas shift reaction than previously anticipated. Hydrocarbon concentrations did not compare favorably with equilibrium calculations, which showed several orders of magnitude in difference. The trends closely matched the ones predicted by equilibrium calculations. The large discrepancy may be accounted for by a re-equilibration of the gas products as they experience three large temperature reductions in the reactor outlet and the sampling system.

6.2 Effectiveness of Sampling Method

The sampling system developed in this study was capable of retaining more gas species than a conventional water impinger based system. In particular, it would allow for the analysis of pentane, butane propane and propylene as well as methyl mercaptan and another possible sulfur containing compound. Additionally, the new sampling system provided several unknown compounds that the gas chromatograph had not been calibrated for. The inclusion of these gases gave a better qualitative analysis for the experiments. Quantitatively, the concentration of minor hydrocarbons also improved, though significant data for confirmation is not present.

The sampling system failed in providing a sample of hydrogen sulfide which from theoretical calculations is the most abundant compound containing sulfur. This indicates that there is still a problem with condensation as hydrogen sulfide is highly soluble in water. The gas chromatograph also incorrectly identified a compound as sulfur dioxide. It is likely that this compound, which shows a connection with methyl mercaptan, may be ethyl mercaptan or dimethyl sulfide, which have similar residence times as sulfur dioxide. Additionally, the gas chromatograph picked up several unknown species, some of which have a similar residence time as carbonyl sulfide. The presence of carbonyl sulfide, ethyl mercaptan and dimethyl sulfide can only be validated by new calibration gases for the gas chromatograph and more testing.

The sampling system performed adequately in identifying the major gas constituents and hydrocarbons but did a poor job at detecting sulfur species, a key objective of this project. It is possible to improve on the system by adding additional heat trace and insulation and monitoring the temperatures more closely. However,

additional revisions to the sampling system do not guarantee detection of hydrogen sulfide.

6.3 Recommendations for Future Work

Experimental testing should continue on the 4-inch fluidized bed gasifier. Additional revisions to the gasifier can be made to increase operational stability and yield better accuracy in the gas composition. The design of the impinger needs to be revisited because it still allows particles and tars to pass through to the filter. This problem can be rectified by increasing the water-to-gas surface area by redesigning it. Additionally, the point at which biomass enters into the system becomes warm and puts stress onto the feeder by the surrounding metal expanding. If the feeder gets too warm, the screws can bind. Including some sort of cooling system will eliminate this stress and prevent biomass from gasifying before entering into the reactor.

The gas chromatograph should be calibrated for carbonyl sulfide, ethyl mercaptan, dimethyl sulfide and carbon disulfide. Further tests should be performed with wood chips to confirm the sulfur compounds present in the syngas stream. The detection of hydrogen sulfide is a critical aspect and should be revisited. The current sampling system can be situated with extra heating and insulation to prevent condensation and the dissolution of hydrogen sulfide. If this problem persists, another method for detecting sulfur will need to be implemented.

APPENDIX A

FEEDER CALIBRATIONS

Table A-1. Calibration of the K-tron feeder for woodchips, based off of 15 minute runs at various set points.

Woodchips (15 min runs) Attached								
	Trial 1			Trial 2			AVG	
Set Point	Net Wgt (g)	Gross Wgt (g)	lbs/hr	Net Wgt (g)	Gross Wgt (g)	lbs/hr	gm/min	lbs/hr
20%	118	87	0.76	119	88	0.77	5.83	0.77±.04
30%	161	130	1.14	162	131	1.15	8.70	1.14±.04
40%	201	170	1.49	205	174	1.53	11.47	1.51±.04
60%	282	251	2.20	286	255	2.24	16.87	2.22±.04
80%	254	223	2.94	255	224	2.95	22.35	2.95±.04
100%	312	281	3.70	309	278	3.66	27.95	3.68±.04

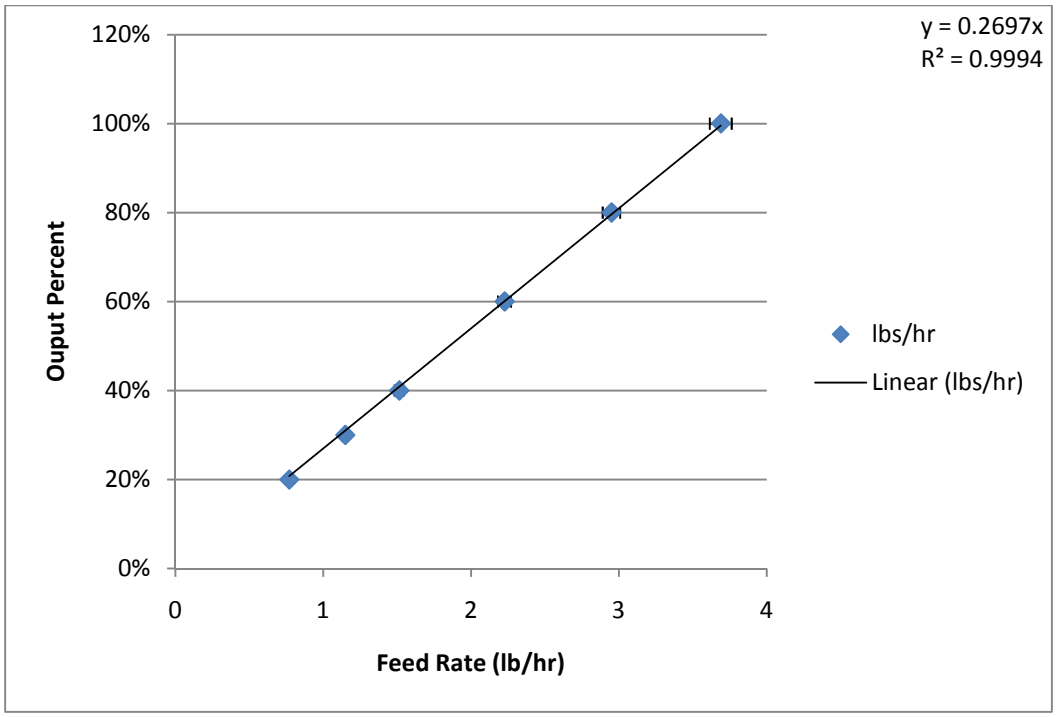

Figure A-1. Plot of the calibration table for woodchips, used to determine precision and the equivalent set point for a specific feed rate.

Table A-2. Calibration of the K-tron feeder for switch grass, based off of 15 minute runs at various set points.

Switch grass (15 min runs) Attached						
	Trial 1		Trial 2		AVG	
Set Point	Net Wgt (lbs)	lbs/hr	Net Wgt (lbs)	lbs/hr	gm/min	lbs/hr
20%	0.81	0.42	0.80	0.36	2.95	0.39±.04
40%	0.89	0.9	0.88	0.84	6.58	0.87±.04
60%	0.985	1.47	0.97	1.38	10.78	1.425±.06
80%	1.075	2.01	1.095	2.13	15.66	2.07±.08
100%	1.17	2.58	1.15	2.46	19.07	2.52±.08

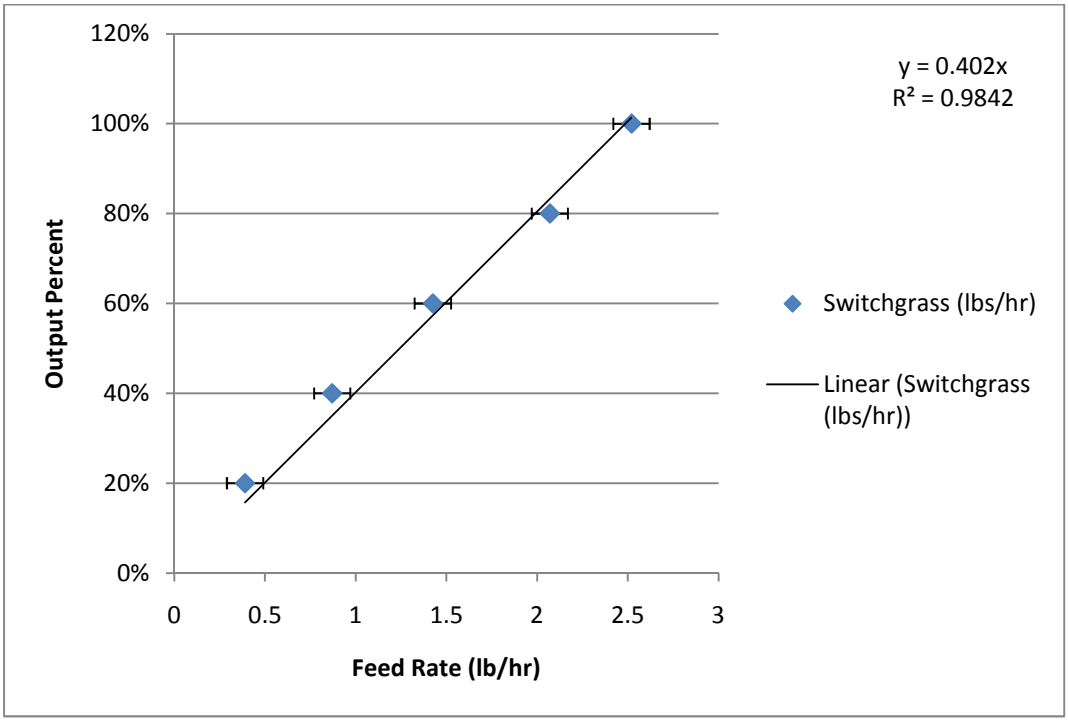

Figure A-2. Plot of the calibration table for switch grass, used to determine precision and the equivalent set point for a specific feed rate.

APPENDIX B

THEORETICAL COMPOSITIONS

Table B-1. Part 1 of the theoretical compounds calculated by Aspen and their respective concentrations as a function of temperature for wood chips.

	H20	C02	CO	H2	O2	CH4	C2H2
°F	Mol Frac	Mol Frac	Mol Frac	Mol Frac	Mol Frac	Mol Frac	Mol Frac
936	0.307	0.242	0.038	0.244	3.84E-28	0.168792	2.01E-13
981	0.282	0.232	0.055	0.285	2.58E-27	0.146061	6.55E-13
1026	0.257	0.218	0.077	0.326	1.55E-26	0.121532	1.87E-12
1071	0.234	0.201	0.102	0.366	8.46E-26	0.096196	4.62E-12
1116	0.214	0.182	0.129	0.402	4.31E-25	0.071552	9.72E-12
1161	0.198	0.164	0.155	0.433	2.1E-24	0.049405	1.72E-11
1206	0.186	0.147	0.178	0.457	9.96E-24	0.031401	2.53E-11
1251	0.180	0.134	0.195	0.473	4.7E-23	0.018404	3.11E-11
1296	0.177	0.123	0.209	0.481	2.2E-22	0.010117	3.31E-11
1341	0.177	0.115	0.218	0.484	1.01E-21	0.005363	3.17E-11
1386	0.180	0.109	0.225	0.483	4.44E-21	0.002814	2.86E-11
1431	0.183	0.104	0.231	0.481	1.86E-20	0.001489	2.51E-11
1476	0.186	0.099	0.236	0.478	7.33E-20	0.000803	2.18E-11
1521	0.190	0.095	0.240	0.474	2.73E-19	0.000442	1.89E-11
1566	0.193	0.091	0.244	0.471	9.6E-19	0.000249	1.64E-11
1611	0.197	0.088	0.247	0.468	3.2E-18	0.000144	1.43E-11
1656	0.200	0.085	0.251	0.465	1.01E-17	8.51E-05	1.25E-11
1701	0.203	0.081	0.254	0.462	3.06E-17	5.14E-05	1.11E-11
1746	0.206	0.079	0.257	0.459	8.82E-17	3.17E-05	9.8E-12
1791	0.209	0.076	0.259	0.456	2.44E-16	1.99E-05	8.73E-12
1836	0.211	0.073	0.262	0.454	6.46E-16	1.27E-05	7.81E-12
1472	0.186	0.100	0.235	0.478	6.63E-20	0.00084	2.2E-11

Table B-2. Part 2 of the theoretical compounds calculated by Aspen and their respective concentrations as a function of temperature for wood chips.

	C2H4	C2H6	C3H6	C3H8	C4H10	S02	H2S
°F	Mol Frac	Mol Frac	Mol Frac	Mol Frac	Mol Frac	Mol Frac	Mol Frac
936	1.71E-08	1.68E-06	1.16E-11	9.57E-11	5.2E-15	1.74E-14	9.53E-05
981	2.65E-08	1.53E-06	1.69E-11	8.67E-11	4.72E-15	2.57E-14	9.19E-05
1026	3.73E-08	1.28E-06	2.15E-11	7E-11	3.68E-15	3.74E-14	8.82E-05
1071	4.66E-08	9.74E-07	2.35E-11	4.9E-11	2.38E-15	5.43E-14	8.44E-05
1116	5.09E-08	6.56E-07	2.12E-11	2.88E-11	1.22E-15	8E-14	8.08E-05
1161	4.77E-08	3.83E-07	1.54E-11	1.37E-11	4.73E-16	1.23E-13	7.76E-05
1206	3.78E-08	1.91E-07	8.82E-12	5.16E-12	1.35E-16	2E-13	7.49E-05
1251	2.54E-08	8.13E-08	4E-12	1.55E-12	1.9E-17	3.5E-13	7.3E-05
1296	1.5E-08	3.06E-08	1.5E-12	3.87E-13	4.76E-18	6.55E-13	7.18E-05
1341	8.13E-09	1.07E-08	5.02E-13	8.7E-14	6.5E-19	1.28E-12	7.11E-05
1386	4.24E-09	3.67E-09	1.6E-13	1.89E-14	8.96E-20	2.52E-12	7.07E-05
1431	2.2E-09	1.27E-09	5.09E-14	4.15E-15	1.25E-20	4.95E-12	7.05E-05
1476	1.15E-09	4.51E-10	1.66E-14	9.51E-16	1.96E-21	9.52E-12	7.04E-05
1521	6.18E-10	1.67E-10	5.63E-15	2.29E-16	3.09E-22	1.79E-11	7.03E-05
1566	3.39E-10	6.39E-11	1.99E-15	5.86E-17	5.28E-23	3.27E-11	7.02E-05
1611	1.9E-10	2.55E-11	7.32E-16	1.58E-17	9.62E-24	5.85E-11	7.02E-05
1656	1.09E-10	1.06E-11	2.81E-16	4.51E-18	1.89E-24	1.02E-10	7.02E-05
1701	6.42E-11	4.55E-12	1.12E-16	1.36E-18	3.93E-25	1.73E-10	7.01E-05
1746	3.86E-11	2.03E-12	4.65E-17	4.28E-19	8.21E-26	2.89E-10	7.01E-05
1791	2.37E-11	9.32E-13	2E-17	1.42E-19	2.12E-26	4.71E-10	7.01E-05
1836	1.48E-11	4.42E-13	8.89E-18	4.9E-20	5.35E-27	7.53E-10	7.01E-05
1472	1.21E-09	4.87E-10	1.8E-14	1.06E-15	2.23E-21	9.07E-12	7.04E-05

Table B-3. Part 3 of the theoretical compounds calculated by Aspen and their respective concentrations as a function of temperature for wood chips.

	CH3SH	C2H6S	C2H6S2	COS	CS2	SO3
°F	Mol Frac	Mol Frac	Mol Frac	Mol Frac	Mol Frac	Mol Frac
936	6.6E-10	4.12E-15	7.4E-22	8.52E-07	2.35E-13	1.87E-26
981	6.87E-10	4.42E-15	8E-22	1E-06	3.49E-13	4.45E-26
1026	6.84E-10	4.37E-15	8.01E-22	1.14E-06	4.99E-13	1.01E-25
1071	6.46E-10	3.91E-15	7.3E-22	1.26E-06	6.84E-13	2.25E-25
1116	5.74E-10	3.11E-15	5.98E-22	1.36E-06	8.98E-13	5.04E-25
1161	4.76E-10	2.16E-15	4.34E-22	1.43E-06	1.13E-12	1.17E-24
1206	3.68E-10	1.29E-15	2.78E-22	1.47E-06	1.38E-12	2.92E-24
1251	2.66E-10	6.74E-16	1.58E-22	1.51E-06	1.62E-12	7.95E-24
1296	1.83E-10	3.14E-16	8.18E-23	1.53E-06	1.86E-12	2.35E-23
1341	1.22E-10	1.37E-16	4.02E-23	1.56E-06	2.1E-12	7.24E-23
1386	8.04E-11	5.84E-17	1.94E-23	1.58E-06	2.35E-12	2.26E-22
1431	5.32E-11	2.51E-17	9.41E-24	1.61E-06	2.6E-12	6.88E-22
1476	3.56E-11	1.1E-17	4.66E-24	1.64E-06	2.86E-12	2.03E-21
1521	2.41E-11	4.97E-18	2.37E-24	1.66E-06	3.14E-12	5.75E-21
1566	1.66E-11	2.32E-18	1.24E-24	1.69E-06	3.42E-12	1.56E-20
1611	1.16E-11	1.11E-18	6.65E-25	1.71E-06	3.72E-12	4.06E-20
1656	8.27E-12	5.53E-19	3.67E-25	1.74E-06	4.04E-12	1.01E-19
1701	5.96E-12	2.82E-19	2.08E-25	1.76E-06	4.36E-12	2.44E-19
1746	4.35E-12	1.48E-19	1.2E-25	1.78E-06	4.7E-12	5.66E-19
1791	3.22E-12	8E-20	7.14E-26	1.8E-06	5.05E-12	1.27E-18
1836	2.41E-12	4.43E-20	4.33E-26	1.82E-06	5.41E-12	2.76E-18
1472	3.66E-11	1.17E-17	4.91E-24	1.64E-06	2.84E-12	1.88E-21

REFERENCES

Avellar, B. K.; Glasser, W. G. Steam-assisted Biomass Fracionation. I. Process Considerations and Economic Evaluation, *Biomass Bioenergy* **1998**, *Vol 14* (3), 205-218.

Bain, R. L. *Thermochemical Technologies for Conversion of Biomass to Fuels and Chemicals*, Biomass to Chemicals and Fuels: Science, Technology and Public Policy, Rice University, Houston, September 26, 2006.

Bain, R. L.; Dayton, D. C.; Carpenter, D. L.; Czernik, S. R.; Feik, C. J.; French, R. J.; Magrini-Bair, K. A.; Phillips, S. D. Evaluation of Catalyst Deactivation during Catalytic Steam Reforming of Biomass-Derived Syngas, *Ind. Eng. Chem. Res.* **2005**, *44*, 7945-7956.

Bartlett, P. D.; Davis, R. E. Reactions of Elemental Sulfur. II. The Reaction of Alkali Cyanides with Sulfur and Some Single-Sulfur Transfer Reactions, *J. Am. Chem. Soc.* Converse Memorial Laboratory of Harvard University, **1958**.

Belgiorno, V.; Feo, G. D; Rocca, C. D.; Napoli, R.M.A. Energy from Gasification of Solid Wastes, *Waste Management* **2003**, *23*, 1-15.

Benson, S. W. *Thermochemistry and Kinetics of Sulfur-Containing Molecules and Radicals,* Department of Chemistry, USC, 1977.

Bridgwater, A. V. The technical and economic feasibility of biomass gasification for power generation, *Fuel* **1995**, *74* (5), 631-653.

Caballero, M. A.; Aznar, M. P.; Gil, J.; Martin, J. A.; Frances, E.; Corella, J. Commercial Steam Reforming Catalysts to Improve Biomass Gasification with Steam-Oxygen Mixtures. 1. Hot Gas Upgrading by the Catalytic Reactor, *Ind. Eng. Chem. Res.* **1997**, *36*, 5227-5239.

Caballero, M. A.; Corella J.; Aznar, M,; Gil, J. Biomass gasification with air in fluidized bed. Hot gas cleanup with selected commercial and full size nickel based catalysts. *Ind. Eng. Chem. Res.* **2000**, *39*, 1143-1154.

Chaudhari, S.T.; Bej, S.K.; Bakhshi, N. N.; Dalai, A.K. Steam Gasification of Biomass-Derived Char for the Production of Carbon Monoxide-Rich Synthesis Gas, *Energy Fuels* **2001**, *15*, 736-742.

Chaudhari, S.T.; Dalai, A.K.; Bakhshi, N. N. Production of Hydrogen and/or Syngas (H2 + CO) via Steam Gasification of Biomass-Derived Chars, *Energy Fuels* **2003**, *17*, 1062-1067.

Ciferno, J. P.; Marano, J. Benchmarking Biomass Gasification Technologies for Fuels, Chemicals and Hydrogen Production, Prepared for U.S. Department of Energy: National Energy Technology Laboratory, 2002.

Collot, A. Matching Gasification Technologies to Coal Properties, *Int. J. Coal Geol.* **2006**, *65*, 191-212.

Cui, H.; Turn, S. Q.; Keffer, V.; Evans, D.; Tran, T.; Foley, M. Contaminant Estimates and Removal in Product Gas from Biomass Steam Gasification, *Energy Fuels* **2010**, *24*, 1222-1233.

Cummer, K. R.; Brown, R. C. Ancillary Equipment for Biomass Gasification, *Biomass Bioenergy* **2002**, *23*, 113-128.

Dasappa, S.; Sridhar, H.V.; Sridhar, G.; Paul, P. J.; Mukunda, H.S. Biomass Gasification-A Substitute to Fossil Fuel for Heat Application, *Biomass Bioenergy* **2003**, *25*, 637-649.

Dayton, D.C.; Jenkins, B. M.; Turn, S. Q.; Bakker, R. R.; Williams, R. B.; Belle-Oudry, B.; Hill, L. M. Release of Inorganic Constituents from Leached Biomass during Thermal Conversion, *Energy Fuels* **1999**, *13*, 860-870.

Delgado, J; Aznar, M. P.; Corella, J. Biomass Gasification with Steam in Fluidized Bed: Effectiveness of CaO, MgO and CaO-MgO for Hot Raw Gas Cleaning, *Ind. Eng. Chem. Res.* **1997**, *36*, 1535-1543.

Delgado, J; Aznar, M. P.; Corella, J. Calcined Dolomite, Magnesite and Calcite for Cleaning Hot Gas from a Fluidized Bed Biomass Gasifier with Steam: Life and Usefulness, *Ind. Eng. Chem. Res.* **1996**, *35*, 3637-3643.

Demirbas, A. Gaseous Products from Biomass by Pyrolysis and Gasification: Effects of Catalyst on Hydrogen Yield, *Energy Convers. Manage.* **2002**, *43*, 897-909.

Draelants, D. J.; Zhao, H.; Baron, G. V. Preparation of Catalytic Filters by the Urea Method and Its Application for Benzene Cracking in H2S-Containing Biomass Gasification Gas, *Ind. Eng. Chem. Res.* **2001**, *40*, 3309-3316.

Dupont, C.; Boissonnet, G.; Seiler, J.; Gauthier, P.; Schweich, D. Study about the Kinetic Processes of Biomass Steam Gasification, *Fuel* **2007**, *86*, 32-40.

Elliott, D. C.; Schiefelbein G. F. Liquid Hydrocarbon Fuels from Biomass, *American Chemical Society, Division of Fuel Chemicals* **1989**, 34 (4), 1160-1166.

Engelen, K.; Zhang, Y.; Draelants, D. J.; Baron, G.V. A Novel Catalytic Filter for Tar Removal from Biomass Gasification Gas: Improvement of the Catalytic Activity in Presence of H2S, *Chem. Eng. Sci.* **2003**, *58*, 665-670.

Evans, W. H.; Wagman, D. D. Thermodynamics of Some Simple Sulfur-Containing Molecules, *J. Res. Natl. Bur. Stan.* **1952**, *49* (3).

Franco, C.; Pinto, F.; Gulyurtlu, I.; Cabrita, I. The Study of Reactions Influencing the Biomass Steam Gasification Process, *Fuel* **2003**, *82*, 835-842.

Fushimi, C.; Araki, K.; Yamaguchi, Y.; Tsutsumi; A. Effect of Heating Rate on Steam Gasification of Biomass. 1. Reactivity of Char, *Ind. Eng. Chem. Res.* **2003**, *42*, 3922-3928.

Fushimi, C.; Araki, K.; Yamaguchi, Y.; Tsutsumi A.; Effect of Heating Rate on Steam Gasification of Biomass. 2. Thermogravimetric-Mass Spectroetric (TG-MS) Analysis of Gas Evolution, *Ind. Eng. Chem. Res.* **2003**, *42*, 3929-3936.

Gangwal, S. K.; Gupta, R.; McMichael, W. J. Hot-Gas Cleanup-Sulfur recovery Technical, Environmental and Economic Issues, *Heat Recovery Syst. CHP* **1995**, *15* (2), 205-214.

Garcia, L.; Salvador, M. L.; Arauzo J.; Bilbao, R. Catalytic Steam Gasification of Pine Sawdust. Effect of Catalyst Weight/Biomass Flow Rate and Steam/Biomass Ratios on Gas Production and Composition, *Energy Fuels* **1999**, *13*, 851-859.

Garcia-Labiano, F.; Hampartsoumian E.; Williams A. Determination of Sulfur Release and its Kinetics in Rapid Pyrolysis of Coal, *Fuel* **1995**, *74* (4), 1072-1079.

Gil J.; Aznar M. P.; Caballero, M. A.; Frances, E.; Corella, J. Biomass Gasification in Fluidized Bed at Pilot Scale with Steam-Oxygen Mixtures. Product Distribution for Very Different Operating Conditions, *Energy Fuel* **1997**, *11* (6).

Gil, J.; Corella J.; Aznar, M. P.; Caballero, M. A. Biomass Gasification in Atmospheric and Bubbling Fluidized Bed- Effect of the type of Gasifying Agent on the Product Distribution, *Biomass Bioenergy* **1999**, *17*, 389-403.

Grabowski, P. *Biomass Thermochemical Conversion OBP Efforts*, U.S. Department of Energy: Office of the Biomass Program, 2004.

Hanaoka, T.; Inoue, S.; Uno, S.; Ogi, T.; Minowa, T. Effect of Woody Biomass Components on Air-Steam Gasification, *Biomass Bioenergy* **2005**, *28*, 69-76.

Hanaoka, T.; Yoshida, T.; Fujimoto S.; Kamei, K.; Harada, M.; Suzuki, Y.; Hatano H.; Yokoyama S.; Minowa, T. Hydrogen Production from Woody Biomass by Steam Gasification using a CO2 Sorbent, *Biomass Bioenergy* **2005**, *28*, 63-68.

Herron, J. T. Thermochemical Data on Gas Phase Compounds of Sulfur Fluorine Oxygen and Hydrogen Related to Pyrolysis and Oxidtion of Sulfur Hexafluoride, *Phys. Chem. Ref. Data,* **1987**.

Higman, C.; Van der Burgt, M. *Gasification*, Elsevier, Burlington, MA 2008.

Hofbauer, H.; Rauch, R.; Foscolo, P.; Matera, D. Hydrogen Rich Gas From Biomass Steam Gasification, Institute of Chemical Engineering, Fuel and Environmental Technology, Getreidemarkt, Vienna, 2000.

Huber, G. W.; Iborra S.; Corma, A. *Synthesis of Transportation Fuels from Biomass: Chemistry, Catalysts and Engineering*, Instituto de Tecnologı´a Quı´micia, Valencia, Spain, 2006.

Kelly, R. A. *Energy Supply and Renewable Resources*, New York, NY: Facts on File, 2007.

Knoef, H. A. M. *Handbook on Biomass Gasification*, BTG Biomass Technology Group B.V., Enschede, The Netherlands, 2010.

Knudsen, J. N.; Jensen, P. A.; Lin, W.; Frandsen, F. J.; Dam-Johansen, K. Sulfur Transformations during Thermal Conversion of Herbaceous Biomass, *Energy Fuels* **2004**, *18*, 810-819.

Koningen, J.; Sjostrom, K. Sulfur-Deactivated Steam Reforming of Gasified Biomass, *Ind. Eng. Chem. Res.* **1998**, *37*, 341-346.

Kumabe, K.; Hanaoka, T.; Fujimoto, S.; Minowa T.; Sakanishi K. Co-gasification of Woody Biomass and Coal with Air and Steam, *Fuel* **2007**, *86*, 684-689.

Lee, Sunggyu *Alternative Fuels*. Taylor & Francis, Washington, D.C., 1996.

Leibold, H.; Hornung A.; Seifert H.; HTHP Syngas Cleaning Concept of Two Stage Biomass Gasification for FT Synthesis, *Powder Technol.* **2008**, *180*, 265-270.

Levine, J. S. *Global Biomass Burning, Atmospheric, Climatic and Biospheric Implications*, Massachusetts Institute of Technology, 1991.

Li, X.T.; Grace, J.R.;.Lim, C.J.; Watkinson, A.P.; Chen H.P.; Kim, J.R. Biomass Gasification in a Circulating Fluidized Bed, *Biomass Bioenergy* **2004**, *26*, 171-193.

Lv, P.M.; Xiong, Z.H.; Chang, J.; Wu, C.Z.; Chen Y.; Zhu, J.X. An Experimental Study on Biomass Air-Steam Gasification in a Fluidized Bed, *Bioresour. Technol.* **2004**, *95*, 95-101.

Maniatis, K. *Progress in Biomass Gasification: An Overview*, Director General for Energy & Transport, Prepared for the European Commission, 2001.

McKendry, P.; Energy Production from Biomass-Gasification Technologies Part 3, *Bioresour. Technol.* **2002**, *83*, 55-63.

McMillen, D. F.; Golden, D. M. Hydrocarbon Bond Dissociation Energies, *Annu. Rev. Phys. Chem.* **1982**, *33*, 493-532.

Miles, T. R.; Miles, T. R. Jr; Baxter L. L.; Breyers, R. W.; Jenkins B. M.; Oden, L. L. Boiler Deposits From Firing Biomass Fuels, *Biomass Bioenergy* **1996**, *10* (2-3), 125-138.

Milne, T. A.; Evans R. J.; Abatzoglou, N. *Biomass Gasifier Tars: Their Nature Formation and Conversion*, National Renewable Energy Laboratory, November 1998.

Mohan, D.; Pittman, C. U. Jr.; Steele, P. H. Pyrolysis of Wood/Biomass for Bio-oil: A Critical Review, *Energy Fuels* **2006**, *20*, 848-889.

Morehead, R.; De Zeeuw, J.; Bromps, B.; Stidsen, G. *Column Selection for Speciation of Sulfur Compounds in Natural Gas*. Bellefonte: Restek Corporation. 2011.

Narvaez, I.; Corella J.; Orio, A. Fresh Tar (from a Biomass Gasifier) Elimination over a Commercial Stem-Reforming Catalyst. Kinetics and Effect of Different Variables of Operation, *Ind. Eng. Chem. Res.* **1997**, *36*, 317-327.

Nordin, A. Optimization of Sulfur Retention in Ash when Cocumbusting High Sulfur Fuels and Biomass Fuels in a Small Pilot Scale Fluidized Bed, *Fuel* **1995**, *74* (4), 615-622.

Olivares, A.; Aznar, M. P.; Caballero, M. A.; Gil, J.; Frances, E.; Corella, J. Biomass Gasification: Produced Gas Upgrading by In-Bed Use of Dolomite, *Ind. Eng. Chem. Res.* **1997**, *36*, 5220-5226.

Olsson, J. G.; Jaglid, U.; Pettersson, J. B. C. Alkali Metal Emission during Pyrolysis of Biomass, *Energy Fuels* **1997**, *11*, 779-784.

Osada, M.; Hiyoshi, N.; Sato, O.; Arai K.; Shirai, M. Effect of Sulfur on Catalytic Gasification of Lignin in Supercritical Water, *Energy Fuels* **2007**, *21*, 1400-1405.

Ponomarev, D.; Takhistov, V. Some Regularities in the Relative Thermodynamic Stabilities of Free Radicals, *J. Mol. Struct.* **1997**, *435*, 259-274.

Rapagna, S.; Jand, N.; Foscolo, P.U. Catalytic Gasification of Biomass to Produce Hydrogen Rich Gas, *Int. J. Hydrogen Energy* **1998**, *23* (7), 551-557.

Rapagna, S.; Jand, N.; Kiennemann A.; Foscolo, P. U. Steam-Gasification of Biomass in a Fluidized-Bed of Olivine Particles, *Biomass Bioenergy* **2000**, *19*, 187-197.

Richardson, J. *Bioenergy from Sustainable Forestry: Guiding Principles and Practice*. Dordrecht u.a.: Kluwer Academic Publ., 2002.

Sadaka, S. S.; Ghaly A. E.; Sabbah, M.A. Two Phase Biomass Air-Steam Gasification Model for Fluidized Bed Reactors: Part I-Model Development, *Biomass Bioenergy* **2002**, *22*, 439-462.

Sato, K.; Fujimoto, K. Development of New Nickel Based Catalyst for Tar Reforming with Superior Resistance to Sulfur Poisoning and Coking in Biomass Gasification, *Catal. Commun.* **2007**, *8*, 1697-1701.

Sato, T.; Osada, M.; Watanabe, M.; Shirai, M.; Arai, K. Gasification of Alkylphenols with Supported Noble Metal Catalysts in Supercritical Water, *Ind. Eng. Chem. Res.* **2003**, *42*, 4277-4282.

Schulz, H.; Short History and Present Trends of Fischer-Tropsch Synthesis, *Appl. Catal., A: General* **1999***, 186*, 3-12.

Schuster, G.; Loffler, G.; Weigl, K.; Hofbauer, H. Biomass Steam Gasification – an Extensive Parametric Modeling Study, *Bioresour. Technol.* **2001**, *77*, 71-79.

Snoeck, J. W.; Froment G. F.; Fowles M. Filamentous Carbon Formation and Gasification: Thermodynamics, Driving Force, Nucleation and Steady-State Growth, *J. Catal.* **1997**, *169*, 240-249.

Srinakruang, J.; Sato, K.; Vitidsant, T.; Fujimoto, K. Highly Efficient Sulfur and Coking Resistance Catalysts for Tar Gasification with Steam, *Fuel* **2006**, *85*, 2419-2426.

Stiegel, G. J.; Maxwell, C. M. Gasification Technologies: The Path to Clean Affordable Energy in the 21st Century, *Fuel Processing Technology* **2001**, *71*, 79-97.

Sutton, D.; Kelleher B.; Ross,J. R. H. Review of Literature on Catalysts for Biomass Gasification, *Fuel Process. Technol.* **2001**, *73*, 155-173.

Tomishige, K.; Asadullah, M.; Kunimori, K. Syngas Production by Biomass Gasification Using Rh/CeO2/SiO2 Catalysts and Fluidized Bed Reactor, *Catal. Today* **2004**, *89*, 389-403.

Tijmensen, M. J. A.; Faaij, A. P. C.; Hemelinck, C. N.; van Hardeveld, M. R. M. Exploration of the Possibilities for Production of Fischer Tropsch Liquids and Power via Biomass Gasification, *Biomass Bioenergy* **2002**, *23*, 129-152.

Turn, S.; Kinoshita, C.; Zhang, Z., Ishimura D.; Zhou, J. An Experimental Investigation of Hydrogen Production from Biomass Gasification, *Int. J. Hydrogen Energy* **1998**, *23* (8), 641-648.

Valmari, T.; Lind, T. M.; Kauppinen, E. I. Field Study on Ash Behavior during Circulation Fluidized-Bed Combustion of Biomass. 1. Ash Formation, *Energy and Fuels* **1999**, *13*, 379-389.

Wang, D.; Czernik, S.; Montane, D.; Mann, M.; Chornet, E. Biomass to Hydrogen via Fast Pyrolysis and Catalytic Steam Reforming of the Pyrolysis Oil or Its Fractions, *Ind. Eng. Chem. Res.* **1997**, *36*, 1507-1518.

Warnecke, R. Gasification of Biomass: Comparison of Fixed Bed and Fluidized Bed Gasifier, *Biomass Bioenergy* **2000**, *18*, 489-497.

Westberg, H. M.; Bystrom M.; Leckner, B. Distribution of Potassium, Chlorine and Sulfur between Solid and Vapor Phases during Combustion of Wood Chips and Coal, *Energy Fuels* **2003**, *17*, 18-28.

Westmoreland, P. R.; Harrison, D. P. Evaluation of Candidate Solids for High-Temperature Desulfurization of Low-Btu Gases, *Environ. Sci. Technol.* **1996**, 10 (7), 659-661.

Xu, X.; Matsumura, Y.; Stenberg J.; Antal, M. J. Jr. Carbon-Catalyzed Gasification of Organic Feedstocks in Supercritical Water, *Ind. Eng. Chem. Res.* **1996**, *35*, 2522-2530.

Yaman, S. Pyrolysis of Biomass to Produce Fuels and Chemical Feedstocks, *Energy Convers. Manage.* **2004**, *45*, 651-671.

Yoshida, T.; Oshima, Y. Partial Oxidative and Catalytic Biomass Gasification in Supercritical Water: A Promising Flow Reactor System, *Ind. Eng. Chem. Res.* **2004**, *43*, 4097-4104.

Yoshida, T.; Oshima Y.; Matsumura Y. Gasification of Biomass Model Compounds and Real Biomass in Supercritical Water, *Biomass Bioenergy* **2004**, *26*, 71-78.

Yrjas, P.; Krisiina, L.; Hupa, M. Limestone and Dolomite as Sulfur Absorbents under Pressurized Gasification Conditions, *Fuel* **1996**, *75* (1), 85-95.